University of Szeged

Albert Szent-Györgyi Medical School

Doctoral School of Theoretical Medicine

PhD Thesis

Controlling cell polarity in human pancreatic organoids significantly improves the resolution of *ex vivo* physiological modeling.

Árpád Varga

Supervisor:

József Maléth MD PhD

Szeged, 2023

1. TABLE OF CONTENTS

2. PUBLICATION RELATED TO THE THESIS

I. Human pancreatic ductal organoids with controlled polarity provide a novel *ex vivo* tool to study epithelial cell physiology - **Árpád Varga,** Tamara Madácsy, Marietta Görög, Aletta Kiss, Petra Susánszki, Viktória Szabó, Boldizsár Jójárt, Krisztina Dudás, Gyula Farkas Jr., Edit Szederkényi, György Lázár, Attila Farkas, Ferhan Ayaydin, Petra Pallagi, József Maléth
Cellular and Molecular Life Sciences (**D1**); MTMT ID: 34024396
IF: 9.261

3. LIST OF PUBLICATIONS NOT RELATED TO THE THESIS

I. Orai1 calcium channel inhibition prevents progression of chronic pancreatitis - Viktória Szabó, Noémi Csákány-Papp, Marietta Görög, Tamara Madacsy, **Árpád Varga**, Aletta Kiss, Balint Tel, Boldizsár Jójárt, Tim Crul, Krisztina Dudás, Mária Bagyánszki, Nikolett Bódi, Ferhan Ayaydin, Shyam Jee, Laszlo Tiszlavicz, Kenneth A. Stauderman, Sudarshan Hebbar, Petra Pallagi, and József Maléth
JCI Insight (**D1**); DOI: https://doi.org/10.1172/jci.insight.167645
IF: 9.484

II. Confinement of Triple-Enzyme-Involved Antioxidant Cascade in Two-Dimensional Nanostructure - Adel Szerlauth*, **Árpád Varga***, Tamara Madácsy, Dániel Sebők, Sahra Bashiri, Mariusz Skwarczynski, Istvan Toth, József Maléth, Istvan Szilagyi
ACS - Materials letters (**D1**); DOI: https://doi.org/10.1021/acsmaterialslett.2c00580
IF: 11.17

III. Thiopurines impair the apical plasma membrane expression of CFTR in pancreatic ductal cells via RAC1 inhibition - Bálint Tél, Noémi Papp, **Árpád Varga**, Viktória Szabó, Marietta Görög, Petra Susánszki, Tim Crul, Aletta Kis, Ingrid H. Sendstad, Mária Bagyánszki, Nikolett Bódi, Péter Hegyi, József Maléth & Petra Pallagi
Cellular and Molecular Life Sciences (**D1**); DOI: https://doi.org/10.1007/s00018-022-04662-y
IF: 9.261

IV. Impaired regulation of PMCA activity by defective CFTR expression promotes epithelial cell damage in alcoholic pancreatitis and hepatitis - Tamara Madácsy, **Árpád Varga**, Noémi Papp, Bálint Tél, Petra Pallagi, Viktória Szabó, Aletta Kiss, Júlia Fanczal, Zoltan Rakonczay Jr., László Tiszlavicz, Zsolt Rázga, Meike Hohwieler, Alexander Kleger, Mike Gray, Péter Hegyi, József Maléth
Cellular and Molecular Life Sciences (**D1**); DOI: https://doi.org/10.1007/s00018-022-04287-1
IF: 9.261

V. Bile acid-and ethanol-mediated activation of Orai1 damages pancreatic ductal secretion in acute pancreatitis - Petra Pallagi, Marietta Görög, Noémi Papp, Tamara Madácsy, **Árpád Varga**, Tim Crul, Viktória Szabó, Melinda Molnár, Krisztina Dudás, Anna Grassalkovich, Edit Szederkényi, György Lázár, Viktória Venglovecz, Péter Hegyi, József Maléth
The Journal of Physiology (**D1**), DOI: https://doi.org/10.1113/JP282203
IF: 5.182

VI. Development of polymer-based multifunctional composite particles of protease and peroxidase activities - Szilárd Sáringer, Tamás Valtner, **Árpád Varga**, József Maléth, István Szilágyi
Journal of Materials Chemistry B (**Q1**); DOI: https://doi.org/10.1039/D1TB01861B
IF: 6.331

VII. Modelling Plasticity and Dysplasia of Pancreatic Ductal Organoids Derived from Human Pluripotent Stem Cells - MarkusBreunig, Jessica Merkle, Martin Wagner, Michael K. Melzer, Thomas F. E. Barth, Thomas Engleitner, Johannes Krumm, Sandra Wiedenmann, Christian M. Cohrs, Lukas Perkhofer, Gaurav Jain, Jana Krüger, Patrick C. Hermann, Maximilian Schmid, Tamara Madácsy, **Árpád Varga**, Joscha Griger, Ninel Azoitei, Martin Müller, Oliver Wessely, Pamela G. Robey, Sandra Heller, Zahra Dantes, Maximilian Reichert, Cagatay Günes, Christian Bolenz, Florian Kuhn, József Maléth, Stephan Speier, tefan Liebau, Bence Sipos, Bernhard Kuster, Thomas Seufferlein, Roland Rad, Matthias Meier, Meike Hohwieler, Alexander Kleger
Cell Stem Cell (**D1**); DOI: https://doi.org/10.1016/j.stem.2021.03.005
IF: 24.633

VIII. TRPM2-mediated extracellular Ca^{2+} entry promotes acinar cell necrosis in biliary acute pancreatitis - Júlia Fanczal, Petra Pallagi, Marietta Görög, Gyula Diszházi, János Almássy, Tamara Madácsy, **Árpád Varga**, Péter Csernay-Biró, Xénia Katona, Emese Tóth, Réka Molnár, Zoltán Rakonczay Jr, Péter Hegyi, József Maléth
The Journal of Physiology (**D1**); DOI: https://doi.org/10.1113/JP279553
IF: 5.182

IX. Intracellular Ca^{2+} Signalling in the Pathogenesis of Acute Pancreatitis: Recent Advances and Translational Perspectives - Petra Pallagi, Tamara Madácsy, **Árpád Varga**, József Maléth
International Journal of Molecular Sciences (**Q1**), DOI: https://doi.org/10.3390/ijms21114005
IF: 5.923

X. Mouse pancreatic ductal organoid culture as a relevant model to study exocrine pancreatic ion secretion – Réka Molnár, Tamara Madácsy, **Árpád Varga**, Margit Németh, Xénia Katona, Marietta Görög, Brigitta Molnár, Júlia Fanczal, Zoltán Rakonczay, Péter Hegyi
Laboratory Investigation (**D1**), DOI: 10.1038/s41374-019-0300-3
IF: 4.197

XI. Ca^{2+} Influx Channel Inhibitor SARAF Protects Mice From Acute Pancreatitis – Aran Son, Malini Ahuja, Daniella M Schwartz, **Arpad Varga**, William Swaim, Namju Kang, Jozsef Maleth, Dong Min Shin, Shmuel Muallem
Gastroenterology (**D1**), DOI: 10.1053/j.gastro.2019.08.042
IF: 17.373

Number of full publications: 12 (2 first author publication)

Cummulative IF: 117.247

4. LIST OF ABBREVIATIONS

CF	Cystic fibrosis
AP	Acute pancreatitis
CP	Chronic pancreatitis
NHE1	Sodium/hydrogen exchanger 1
NBC	Sodium/bicarbonate cotransporter
SLC26A6	Anion exchanger
NHE3	Sodium/hydrogen exchanger 3
LGR5	Leucine-rich repeat-containing G-protein coupled receptor 5
CFTR	Cystic fibrosis transmembrane conductance regulator
EHS	Engelbreth-Holm-Swarm mouse sarcomas
CF	Cystic fibrosis
KRT19	Cytokeratin 19
OCLN	Occludin
SOX9	SRY-Box transcription factor 9
EPCAM	epithelial cell adhesion molecule
CDH1	E-cadherin
HES1	Hes family BHLH Transcription Factor 1
AMY1A	Amylase alpha 1A
AMY1B	Amylase alpha 1B
AMY1C	Amylase alpha 1C
PPY	Pancreatic polypeptide
INS	Insulin
CHGA	Chromogranin A
CHGB	Chromogranin B
CDH5	Vascular endothelial cadherin
VIL1	Villin
PLS1	Plastin1
ESP	Espin1
ACTG1	Actin gamma 1
MYO1A	Myosin 1A
MYO6	Myosin 6
EZR	Ezrin
SLK	STE20 like kinase
MYO7B	Myosin 7 B
USH1C	Harmonin
PIEZO1	Piezo-Type Mechanosensitive Ion Channel Component 1
CCNA1	Cyclin A1
CCNA2	Cyclin A2
CCNB1	Cyclin B1
CCNB2	Cyclin B2
CCNB3	Cyclin B3
CCND1	Cyclin D1

CCND2	Cyclin D2
CCND3	Cyclin D3
CCNE1	Cyclin E1
CCNE2	Cyclin E2
CCNQ	Cyclin M
ANO1-10	Anoctamin 1-10
SCNN1A	Sodium channel epithelial 1 subunit alpha
SCNN1B	Sodium channel epithelial 1 subunit beta
SCNN1D	Sodium channel epithelial 1 subunit delta
SCNN1G	Sodium channel epithelial 1 subunit gamma
ATP2B1	ATPase Plasma Membrane Ca^{2+} Transporting 1
ATP2B2	ATPase Plasma Membrane Ca^{2+} Transporting 2
ATP2B3	ATPase Plasma Membrane Ca^{2+} Transporting 3
ATP2B4	ATPase Plasma Membrane Ca^{2+} Transporting 4
ATP2A1	ATPase Sarcoplasmic/Endoplasmic Reticulum Ca^{2+} Transporting 1
ATP2A2	ATPase Sarcoplasmic/Endoplasmic Reticulum Ca^{2+} Transporting 2
ATP2A3	ATPase Sarcoplasmic/Endoplasmic Reticulum Ca^{2+} Transporting 3
STIM1	Stromal Interaction Molecule 1
STIM2	Stromal Interaction Molecule 2
ORAI1	ORAI Ca^{2+} Release-Activated Calcium Modulator 1
ORAI2	ORAI Ca^{2+} Release-Activated Calcium Modulator 2
ORAI3	ORAI Ca^{2+} Release-Activated Calcium Modulator 3
CAMK2A	Ca^{2+}/Calmodulin dependent protein kinase II alpha
CAMK2B	Ca^{2+}/Calmodulin dependent protein kinase II beta
CAMK2D	Ca^{2+}/Calmodulin dependent protein kinase II delta
CAMK2G	Ca^{2+}/Calmodulin dependent protein kinase II gamma
AE	Anion exchanger
AQP	Aquaporin
TJ	Tight junction

5. INTRODUCTION

5.1. Pancreatic ductal ion and fluid secretion

The pancreas is an upper abdominal organ of the digestive system consisting of two main distinct but essential parts, the endocrine and exocrine pancreas. As an endocrine gland, pancreas regulates blood sugar levels by secreting somatostatin, glucagon, pancreatic polypeptide and insulin, resulting in strictly regulated blood glucose concentrations, in the range of 4.0-6.0 mmol/l in normal conditions. As the part of the digestive system, the exocrine pancreas consists of duct cells forming a tree-like brunching system, secreting around 2 L of HCO_3^- rich alkaline fluid daily in order to wash out bioactive molecules to the duodenum, included digestive enzymes produced by acinar cells which are the second major pancreatic exocrine cell type [1]. Exocrine epithelial cells not only act as a barrier and govern ion and fluid secretory processes to maintain organ homeostasis but preventing early proenzyme activation and thus tissue damage or failure [1–3]. On the other hand, impaired ductal secretion is a common feature in distinct pathophysiological conditions of the pancreas such as the genetic disorder cystic fibrosis (CF) and acute (AP) or chronic pancreatitis (CP) [4–8]. The vectorial ion and fluid secretion of the ductal cells are essentially determined by the expression pattern and localization of ion channels and transporter proteins that display a strictly organized apical-to-basal polarity (**Figure 1**.) [1,9].

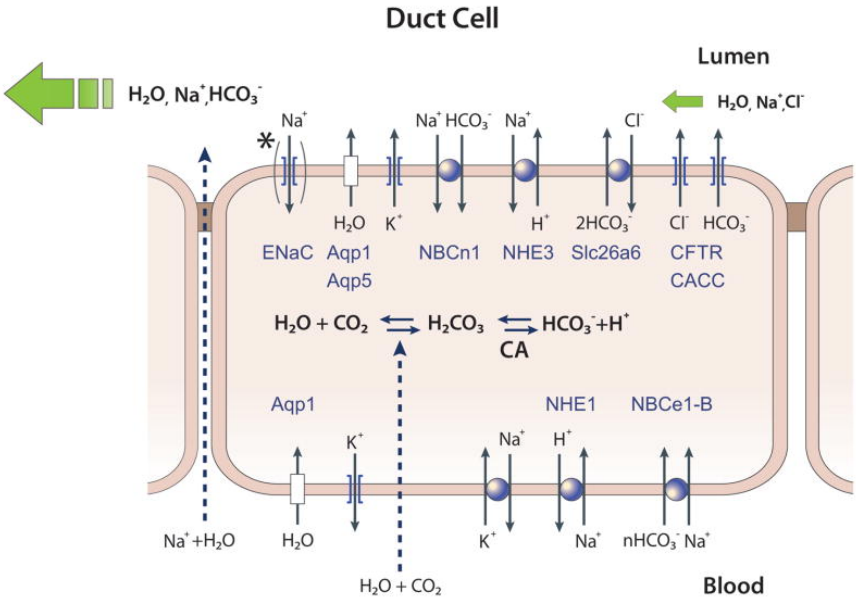

Figure 1. Schematic representation of the pancreatic and salivary ductal fluid and HCO_3^- secretion. Main transporters in the basolateral and luminal membranes mediating HCO_3^- secretion of ductal cells are indicated such as NHE1, NBCe1-B, CFTR-Slc26a6 complex, NBCn1 and NHE3. According to Lee et al. (2012), the salivary, but not the pancreatic, duct also expresses ENaC at the luminal membrane (*) [1].

According to the currently accepted model of ion secretion, the pancreatic ductal cells express the cystic fibrosis transmembrane regulator (CFTR) Cl^- channel and SLC26A6 Cl^-/HCO_3^- exchanger on the apical membrane (**Figure 1.**) [1]. The functional interplay of these proteins and physical interaction of the R domain of CFTR and STAS domain of SLC26A6 enable the pancreatic ductal cells to generate a remarkably high intraluminal HCO_3^- concentration that is ~140 mM in humans [10]. However, due to the limitations of the currently available model systems, the details of human pancreatic HCO_3^- secretion, including the role of ENaC or other Cl^- channels such as ANO1, are still controversial and not fully understood.

5.2. *In vitro*/*ex vivo* model systems for investigating pancreatic ion and fluid secretion

The major bottleneck in the study of pancreatic secretory processes is the lack of human-relevant model systems that provide access to the apical membrane of ductal cells. Although, adherent cell lines and animal models are widely used and universal tools in both basic research and biomedical drug discovery they all have certain limitations[11]. Due to frequent species-specific differences, extrapolation of results from models or clinical translation of basic research findings remained a major unmet need.

One of the first *in vitro* models to explore secretion mechanisms was an adherent human ductal adenocarcinoma (PDAC) cell line, the CAPAN-1 which recapitulate the basic properties of ductal cells[12]. H.S. Cheng et. al in 1998 showed that PDAC cells with human origin are capable of secreting both Cl^- and HCO_3^- concurrently and independently. Later studies have shown that CAPAN-1 expresses key elements of the secretion machinery, such as CFTR and ANO1, which has paved the way for modelling pathological processes [13,14]. The initial results with PDAC cell lines were promising, but there were reasonable concerns about the implications of applying the conclusions drawn from tumor cell lines carrying various mutations (*KRAS*, *TP53* etc.) to primary healthy cells.

They have therefore been almost completely overshadowed by the standardized isolation procedure of murine pancreatic ductal fragments allowing access to primary epithelial cells [15]. The isolation of pancreatic ductal fragments is based on enzymatic digestion of pancreatic tissue by collagenase and manual microdissection of the fragments by stereomicroscope. This technique is still extensively used to study the physiology and pathology of pancreatic ductal epithelium [16–19]. Since the isolated ductal fragments show a heterogeneous cellular composition (epithelial cells, mesenchymal cells, immune cells, blood cells and fibroblasts) with limited cell numbers, high-throughput methods are difficult or impossible to apply on them. Moreover, both

gene expression and functional measurements can be affected by the mixed culture, which can easily result in misleading conclusions.

It has been reported previously that *ex vivo*, 3-dimensional epithelial organoid cultures (OCs) can be established by maintaining WNT and bone morphogenetic protein (BMP) signal transduction pathways in leucine-rich repeat-containing G-protein coupled receptor 5 (LGR5) positive adult stem cells of the gastrointestinal tract [20]. OCs which shows high self-renewal capacity in general opened up new horizons for 3-dimensional model systems although their application possibilities are at an early stage [21–24]. The recently developed patient-derived organoid cultures may provide a physiologically more relevant platform resolving previous difficulties [25–27].

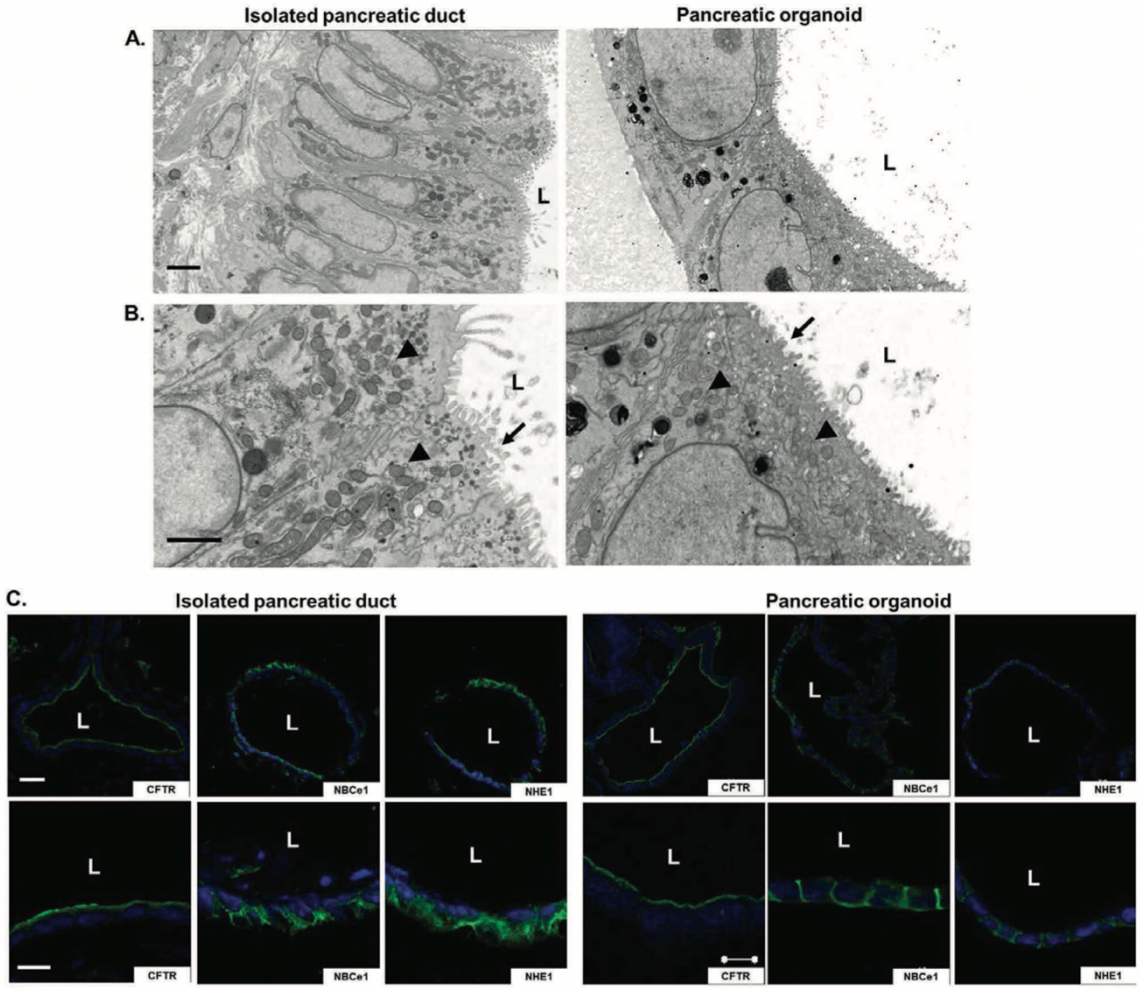

Figure 2. Comparison of polarized epithelial cell layer in isolated pancreatic ductal fragments and organoids. The figure provided by Molnár et al shows the similarity of ultrastructure of epithelial cells in isolated ducts and pancreatic organoids using scanning electron microscopy technique (A-B.) and demonstrate the identical polarized localization of CFTR, NBCe1 and NHE1 by immunofluorescent labeling (C.) [21].

Our group previously demonstrated that the expression, localization and function of key proteins involved in ductal fluid and ion secretion (CFTR, Na^+/H^+ exchanger 1. – NHE1 and electrogenic Na^+/HCO_3^- cotransporter 1 – NBCe1) are equivalent in the pancreatic organoids and the primary isolated ductal fragments in mice (**Figure 2.**) [21]. Moreover, the HCO_3^- secretion and CFTR activity is equivalent in the pancreatic organoids and the isolated ductal fragments. However, direct accessibility of the apical membrane which would be essential for basic physiological investigations and to develop drug screening assays is still difficult to implement. In addition, due to the vectorial ion and fluid transport into the lumen of the organoids, the increasing intraluminal pressure alone may be sufficient to negatively regulate epithelial secretory or barrier functions via Piezo1 mechanosensitive receptor [28]. One possible strategy to overcome this could be the manipulation of the cell polarity in organoids, which was successfully applied in intestinal and airway organoids by the removal of the extracellular matrix (ECM) to investigate host-pathogen interactions and infectious diseases [29–31]. However, it is currently unknown how the polarity switch may alter epithelial cell functions.

5.3. Basic principles of maintaining pancreatic ductal organoid cultures

Pancreatic organoids can be generated from isolated ductal fragments by embedding them in a so-called extracellular membrane matrix such as Matrigel and by using a special culturing medium [32]. Matrigel is traditionally isolated from Engelbreth-Holm-Swarm (EHS) mouse sarcomas in which extracellular matrix elements are significantly enriched. The isolation mixture contains approximately 60% laminin, 30% collagen IV and 8% entactin which provides a perfect model of the basement membrane that contacts with the basal layer of epithelial cells or endothelial cells in the physiological tissue environment. OCs maintenance is also highly dependent on the applied cultured media which supposed to promote cell division by inducing WNT pathway. Essential components of organoid culturing media are a series of growth factors that include R-spondin and antagonists of BMP signaling such as Noggin. Therefore, OC feeding media is mainly produced now by L-WRN cell cultures which were originally derived from L-WNT3A cell line with co-expressing vectors of R-spondin 3 and Noggin. Stable clone selection is continuously maintained in culture by applying G418 and Hygromicyn B. L-WRN cells secrete Wnt3A, R-spondin 3 and Noggin into the medium in which conditioned media is used to culture organoids. While Wnt3A binds to members of the frizzled receptor family and activates β-catenin-dependent transcription, members of the R-spondin protein family are potent coactivators of canonical Wnt signaling, whereas noggin is a bone morphogenetic protein (BMP) signaling inhibitor (**Figure 3.**).

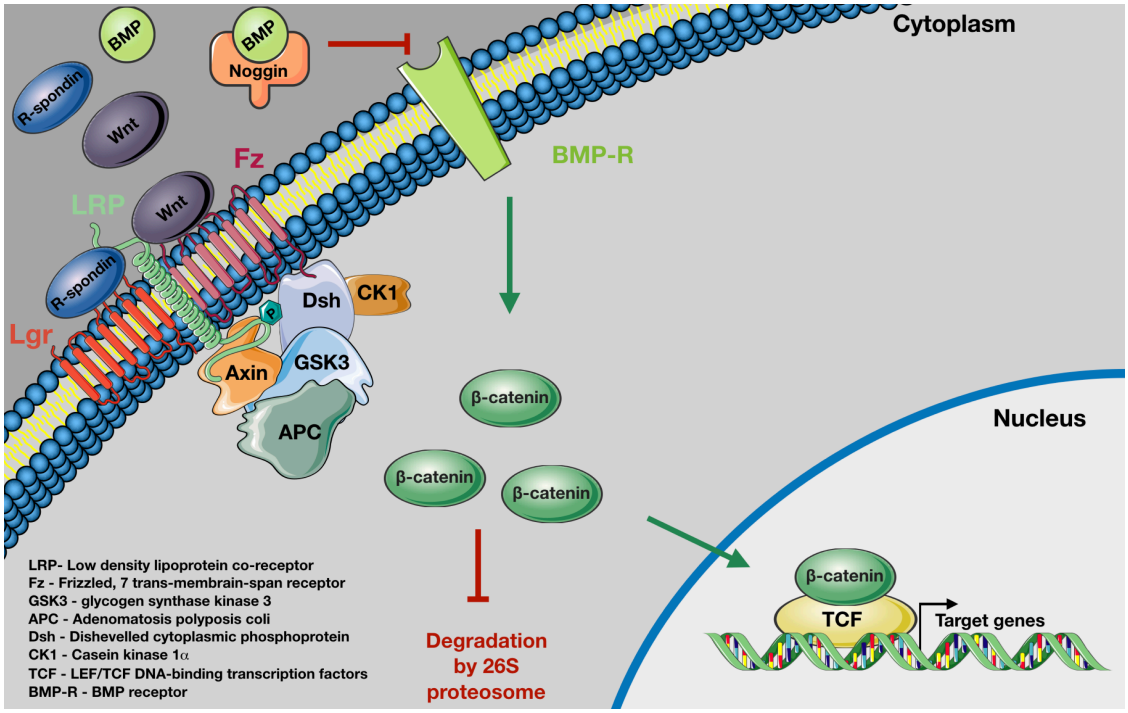

Figure 3. Schematic figure highlights of the effect of main components of the OC medium resulted in induced WNT signaling pathway. WNT and R-spondins has a high affinity to Lgr and Fz receptors to induce canonical WNT pathway while Noggin promotes this effect by inhibiting BMP ligands.

This technique has been also used successfully to establish and maintain patient-derived pancreatic organoids in culture to further study cystic fibrosis (CF) related disorders *in vitro* with a co-culturing system [33]. The results so far are very promising, however, the manual isolation of ductal fragments makes standardization and even future automatization difficult. Moreover spherical-like structure of the organoids, and thus the difficulty in accessing the apical side and therefore the apical channels and transporter playing role in secretory processes, still poses a challenge.

5.4. Perplexity and open questions about the mechanisms of pancreatic ion secretion

Traditionally, transepithelial Na^+ transport occurs in two steps, first luminal sodium crosses the apical plasma membrane by electrodiffusion along its electrochemical gradient and second, subsequent Na^+ extrusion into the interstitial space by the basolateral pumps such as Na^+, K^+-ATPase (**Figure 1.**). ENaC is responsible for absorption of sodium in several epithelium including kidney and salivary gland and has been molecularly characterized as a hetero-oligomeric protein consisting of a 1:1:1 stoichiometry of α (*SCNN1A)*, β (*SCNN1B)*, and γ (*SCNN1G)* subunits[1,34,35]. Channel structure is composed of a large extracellular domain and a narrow transmembrane domain.

In the intestinal, kidney or respiratory epithelia, ENaC is generally co-expressed along with CFTR HCO_3^- and Cl^- channel which proposed to inhibit the function of ENaC. Moreover, deletion of CFTR lead to increased ENaC activity in vitro resulting in lead to airway surface liquid and mucus dehydration that causes mucus obstruction, neutrophilic infiltration, and chronic bacterial infection [36–38]. However, in other epithelia such as in the salivary gland, deletion of CFTR led to inhibited sodium uptake and interestingly, the inhibition of ENaC function significantly reduced CFTR mediated Cl^- absorption. Moreover, CFTR KO resulted in almost distinguished α ENaC expression [39]. Studies showing the interactions of CFTR and ENaC may seem rather controversial, but their interplay regardless of tissue specificity draws attention to the relationship between them in various organ.

The pancreas is one of the organs strongly affected by CF with major dysfunction in Cl^- and HCO_3^- secretion, which is mainly govern by CFTR. Although the pancreas as well as the brain, testis and ovary have previously been shown to contain δ-ENaC subunit transcripts, and ENaC transcripts have been also detected in the human pancreas, an *in vivo*/*in vitro* study on rat pancreatic cells shows that pancreas especially pancreatic ducts do not express functional ENaC, which seems to be a generally accepted finding. [40–42].

Another controversial area has emerged around the role of the ANO1 (*TMEM16A*), which act as a calcium-activated chloride channel (CaCC) [43,44]. As a Cl^- channel, ANO1 plays an important role in regulating the luminal pH in exocrine acinar cells, and also interacts with CFTR to participate in insulin secretion and exocytosis in endocrine beta cells [45,46]. In addition to the role of ANO1 as a Cl^- channel, studies have suggested that ANO1 also has a dynamically regulated permeability to HCO_3^- and may therefore play an important role in transepithelial HCO_3^- secretion [45,47]. Although it was previously agreed that in exocrine tissues ANO1 is expressed in acinar but not in ductal cells, in recent years this seems to be contradicted, as ANO1 expression has been reported from both pancreatic ductal cells and pancreatic adenocarcinoma cell lines [1,48,49].

Since both ENaC and ANO1 are potential therapeutic targets in CF and pancreatitis, there is considerable interest in developing drugs targeting them. Ductal organoids may also provide the opportunity to study the physiology of both channels at higher resolution and accelerate the development of compounds designed to modulate the functions of ENaC or ANO1.

6. AIMS

We aimed to set up an optimized enzymatic digestion-based cell isolation protocol for establishing OCs which could be the next step in standardization and future automatization of the procedure.

We also aimed to establish an advanced culturing method for human pancreas derived organoids based on ECM-removal-induced apical-to-basal polarity switching in order to investigate ion and fluid secretion.

Further goals include investigating the effect of polarity switching on the Ca^{2+} homeostasis of human pancreas organoids.

7. MATERIALS AND METHODS

7.1. Preparation of L-WRN conditioned media

L-WRN cell line was grown in selection medium containing 10% FBS and 0.5-0.5 mg/ml G418 and Hygromycin B in ATCC-formulated DMEM [50]. The conditioned medium supplemented with 10% FBS and 1-1% kanamycin-sulfate and antibiotic-antimycotic solution and has been collected three times from the date of plating every three days and pooled and aliquoted before further applications to minimalize batch-to-batch variation. L-WRN conditioned media has been stored at -20°C prior application for no longer than a month. Materials are listed in **Table 1**.

L-WRN conditioned media		
Component	Manufacturer	Cat.No.
L-WRN cell line	ATCC	ATCC-CRL-3276
FBS	Gibco	10500064
G-418	Gibco	11811031
Hygromycin B	Invitrogen	10687010
ATCC-formulated DMEM	ATCC	ATCC-30-2002
Kanamycin Sulfate	Gibco	15160054
Antibiotic-Antimycotic (100X)	Gibco	15240062

Table 1. Composition of L-WRN conditioned media.

7.2. Generation/maintenance and polarity-change induction of human pancreas OCs.

Human pancreatic tissue samples were collected from cadaver donors (Ethical approval No.: 37/2017-SZTE). Establishment and maintenance protocols were described previously [50]. Briefly, collected tissue samples were placed in splitting media **(Table 2.)** and enzymatic digestion at 37°C was performed in digestion media **(Table 3.)**.

Generation/maintenance and polarity-change induction of human pancreas OCs.		
Spitting media		
Component	Manufacturer/Cat.No.	Final cc/volume
Advanced DMEM/F-12	Gibco, Catalog No.: 12634-010	500 ml
1 M HEPES	Gibco, Catalog No.: 15630080	5 ml (10 mM)
GlutaMax Supplement(100X)	Gibco, Catalog No.: 35050061	5ml (1X)
Primocin (400X)	Invivogen, Catalog No.: ant-pm-2	1,25 ml (1X)

Table 2. Composition of splitting media.

Generation/maintenance and polarity-change induction of human pancreas OCs.		
Digestion Media		
Component	Manufacturer/Cat.No.	Final cc/volume
Splitting media	-	19,0984 ml
Collagenase IV.	Worthington, Catalog No.: LS004188	1250 U/ml
Dispase	Sigma-Aldrich, Catalog No: D4693-1G	0,5 U/ml
FBS	Gibco, Catalog No: 10500064	0,5 ml 2,5%
Soybean Trypsin Inhibitor	Sigma-Aldrich, Catalog No: T9128-1G	1mg/ml
Kanamycin Sulfate	Gibco, Catalog No: 15160054	200 µl 1X
Antibiotic-Antimycotic Solution	Gibco, Catalog No: 15240062	200 µl 1X
Voriconazole (25mg/ml)	Tocris, Catalog No: 3760/10	1,6 µl (cc:2 µg/ml)

Table 3. Composition of digestion media.

Efficiency of the tissue digestion was verified by stereomicroscopy every 10 minutes. The digested cell suspension was centrifuged (200 RCF, 10 min, 4ºC, Rotor radius: 180 mm) and the pellet was washed 3 times in total in wash media **(Table 4.)** and resuspended in Matrigel.

Generation/maintenance and polarity-change induction of human pancreas OCs.		
Wash Medium		
Component	Manufacturer/Cat.No.	Final cc/volume
Splitting media	-	47,7484 ml
FBS	Gibco, Catalog No: 10500064	1,25 ml (2,5%)
Kanamycin Sulfate	Gibco, Catalog No: 15160054	500 µl (1X)
Antibiotic-Antimycotic Solution	Gibco, Catalog No: 15240062	500 µl (1X)
Voriconazole (25mg/ml)	Tocris, Catalog No: 3760/10	4 µl (cc:2 µg/ml)

Table 4. Composition of wash media.

10 µl Matrigel was placed in each well of a 24-well cell culture plate and left for 10 minutes for solidification at 37ºC and 500 µl feeding media was applied in each well **(Table 5.)**. For culture splitting/subculturing, Matrigel removal and cell separation were performed simultaneously by using a 25V/V% TrypLE™ Express Enzyme in DPBS at 37ºC for 15-20 minutes in a vertical shaker followed by two times washing and plating steps as described above. Polarity change of fully grown organoids was induced by extracellular matrix removal with a 7-minute-long treatment of previously described digestion media **(Table 3.)** at 37ºC

followed by two gentle washing steps (parameters of centrifugation: 8 RCF, 10 min, 4ºC, Rotor radius: 180 mm). Organoids with retained cystic structure were replaced in 6-well plates pre-treated with Anti-Adherence Rinsing Solution and fed with feeding medium described above. All applied materials are listed in **Table 2-6**.

Generation/maintenance and polarity-change induction of human pancreas OCs.		
Feeding Medium		
Component	Manufacturer/Cat.No.	Final cc/volume
Splitting media	-	22,808 ml
A-83	TOCRIS, Catalog No: 2939	500 nM (50 µl)
EGF	Gibco, Catalog No: PMG8041	50 ng/ml (5 µl)
FGF	Gibco, Catalog No: PHG0360	100 ng/ml (5 µl)
Gastrin I	TOCRIS, Catalog No: 3006	0.01 µM (5 µl)
N-acetylcysteine	Sigma-Aldrich, Catalog No: A9165-56	1.25 mM (125 µl)
Nicotinamide	Sigma-Aldrich, Catalog No: NO636-100G	10 mM (500 µl)
B-27 Supplement (50X)	Gibco, Catalog No: 17504001	1X (1ml)
L-WRN conditioned media	-	25 ml
Y-27632 Rho-Kinase Inhibitor	TOCRIS, Catalog No: 1254	10.5 µM (50 µl)
Prostaglandin E2 (PGE2)	TOCRIS, Catalog No: 2296	1 µM (50 µl)
Kanamycin Sulfate	Gibco, Catalog No: 15160054	1X (500 µl)
Antibiotic-Antimycotic Solution	Gibco, Catalog No: 15240062	1X (500 µl)
Voriconazole (25mg/ml)	Tocris, Catalog No: 3760/10	4 µl (cc:2 µg/ml)

Table 5. Composition of feeding media.

Generation/maintenance and polarity-change induction of human pancreas OCs.		
Component	Manufacturer	Cat.No.
Matrigel	Corning	354234
24-well plate	Greiner	662160
TrypLE™ Express Enzyme	Gibco	12605028
Anti-Adherence Rinsing Solution	StemCell Technologies	07010

Table 6. Additional materials for OCs culturing and polarity-switch induction.

7.3. Cryopreservation of primary epithelial cells

For cryopreservation organoids were digested to single-cell suspension by TrypLE™ Express Enzyme as described above. After 3 washing steps (50 RCF, 5 min, 4ºC, Rotor radius: 180 mm) the cell pellet was resuspended in Cryo medium based on feeding media and supplemented with

40% FBS and 5% DMSO. Cells were frozen in a propanol filled container (Nalgene Mr. Frosty, Sigma, C1562) according to the manufacturer's protocol and stored in liquid nitrogen long-term. Materials are listed in **Table 7**.

Cryopreservation of primary epithelial cells		
Component	Manufacturer	Cat.No.
DMSO	Sigma	D5879-1L
2-Propanol	Molar Chemicals	00390
Mr. Frosty	Sigma	C1562

Table 7. Listed materials for cryopreservation of primary epithelial cells.

7.4. siRNA transfection of apical-out hPOCs

Apical-out hPOCs were transfected with 50 nM siRNA or siGLOGreen transfection indicator and Lipofectamine 2000 in Feeding media **(Supplementary Table 5)** for 48h. Pre-designed and validated siRNA sets used for gene specific knockdown are listed in **Table 8**.

siRNA transfection of apical-out hPOCs		
Component	Manufacturer	Cat.No.
siGLO Green transfection indicator	Horizon	D-001630-01
Lipofectamine 2000	Invitrogen	11668019
Opti-MEM	Gibco	31985070
CFTR siRNA pool	Dharmacon	L-006425-00-0005
ANO1 siRNA poo	Dharmacon	L-027200-00-0005
SCNN1A siRNA pool	Dharmacon	L-006504-00-0005
SCNN1D siRNA pool	Dharmacon	L-006506-00-0005

Table 8. Listed materials for siRNA transfection.

7.5. Gene expression analysis by qRT-PCR method for validating siRNA-based knock-down efficiency

Apical-in and apical-out hPOCs were used for RNA purification by NucleoZOL reagent. RNA concentration and purity of the samples were checked by NanoDrop spectrophotometer. In total, 1 µg purified mRNA was used for cDNA synthesis which was carried out by iScript cDNA Synthesis kit. RT-PCR reactions were performed by SsoAdvanced Universal SYBR Green Supermix and *CFTR, ANO1, SCNN1A/D* and *B2M* cDNA-specific primers. Relative gene expression analysis was performed by ΔΔCq technique. All the applied primers sets and reagents are listed in **Table 9-10**.

Gene expression analysis by qRT-PCR method for validating siRNA-based knock-down efficiency		
Component	Manufacturer	Cat.No.
NucleoZOL	Macherey-Nagel	740404
NanoDrop One/OneC UV-Vis Spectrophotometer	Thermo Scientific	ND-ONEC-W
iScript cDNA Synthesis kit	Bio-Rad	1708890
SsoAdvanced Universal SYBR Green Supermix	Bio-Rad	1725274

Table 9. Listed materials for cryopreservation of primary epithelial cells

Gene expression analysis by qRT-PCR method for validating siRNA-based knock-down efficiency		
Gene	Fwd (5'-3')	Rev (5'-3').
CFTR	CTGGAGCAGGCAAGACTTCA	TTGGCATGCTTTGATGACGC
ANO1	TCACCAAGATCGAGGTCCCA	GCCACGTAAAAGATGGGGGT
SCNN1A	CCTGCAACCAGGCGAATTAC	ACCGTTGTTGATTCCAGGCA
SCNN1D	TGGGGTTCAGACTGTGCAA	CAGTCCAGGCCATCGTAACT
B2M	TGGAGGCTATCCAGCGTACT	CTCTGCTGGATGACGTGAGT

Table 10. Details of applied primer pairs for qRT-PCR method.

7.6. Gene expression analysis of hPOCs by RNA-Seq

RNA was extracted from collected cell pellet by NucleoSpin RNA Plus kit according to the manufacturer's protocol **(Table 11.)**. RNA-sequencing performed by Illumina NextSeq 500 instrument and data analyses process service were provided by DeltaBio2000 Ltd. Gene expression pattern was determined according to TPM (transcript/million) values.

Gene expression analysis of hPOCs by RNA-Seq		
Component	Manufacturer	Cat.No.
NucleoSpin RNA Plus kit	Macherey-Nagel	740984.250

Table 11. Details of the applied kit for RNA isolation.

7.7. Immunofluorescent labelling and confocal microscopy

Immunofluorescent labelling on organoid cross sections was performed as previously described [50]. Briefly, organoids were frozen and sectioned in Shandon™ Cryomatrix™ at -20 °C. Sections (7 µm thick) were placed on microscope slides. Samples were fixed 4% PFA-PBS for 20 minutes followed by washing for 3x5 minutes in PBS. Antigen retrieval was performed in Sodium Citrate - Tween20 buffer (0.001 M Sodium Citrate Buffer, pH 6.0 and 0.05% Tween20) at 94 °C for 30 min followed by blocking step with 0.1% goat serum and 10% BSA in PBS for 2 hours at 37°C. Primary antibodies were applied overnight at 4°C while secondary antibodies

were incubated for 2 hours at room temperature. Nuclear staining and mounting carried out simultaneously by ProLong™ Gold Antifade mounting medium with DAPI. Images were captured by a Zeiss LSM880 confocal microscope using a 40X oil immersion objective (Zeiss, NA: 1.4). Antibodies and materials applied are listed in **Table 12**.

Immunofluorescent labeling for confocal microscopy		
Component	Manufacturer	Cat.No.
Shandon Cryomatrix	ThermoFisher S.	6769006
Cryostat	Leica	CM 1860 UV
Microscope slides	ThermoFisher S.	J3800AMNZ
PFA	Alfa Aesar	43368
PBS	Sigma	P4417-100TAB
Sodium Citrate	Sigma	71402
Tween-20	Sigma	P1379
Goat Serum	Sigma	G9023
Bovine Serum Albumin (BSA)	Pan-Biotech	P061391100
Anti-CFTR antibody	Abcam	ab2784
Cytokeratin 19 Antibody	ThermoFisher S.	MA5-31977
Anti-SLC4A4/NBC	Abcam	ab187511
Occludin Monoclonal Antibody	ThermoFisher S.	33-1500
Recombinant Anti-SOX9 antibody	Abcam	ab185966
Phalloidin	Abcam	ab176759
Anti-HNF-1B antibody	Abcam	ab236759
Recombinant Anti-FOXA2 antibody	Abcam	ab108422
DOG-1 antibody	ThermoFisher S	MA5-16358
alpha-ENaC antibody	ThermoFisher S	PA1-920A
Extracellular Anti-Orai1 antibody	Alomone Labs	ACC-062
Anti-PIEZO1 antibody	Alomone Labs	APC-087
Goat anti-Mouse Alexa 488	ThermoFisher S.	A11001
Goat anti-Rabbit Alexa 488	ThermoFisher S.	A11034
Donkey anti-Mouse Alexa 647	ThermoFisher S.	A31571

Table 12. Listed materials applied for immunofluorescent labeling and confocal microscopy

7.8. Scanning Electron Microscopy

Organoids were fixed with 2.5% (v/v) glutaraldehyde and 0.05 M cacodylate buffer (pH 7.2) in PBS overnight at 4 ◦C. 8 µL samples spotted onto a silicon disc coated with 0.01% (w/v) poly-l-lysine. Discs were washed twice with PBS and dehydrated with a graded ethanol series (30%, 50%, 70%, 80%, 100% ethanol (v/v), for 2 h each at 4 ◦C and 100% EtOH, for overnight). Following dehydration, samples were immersed for 5 mins in pure hexamethyldisilazane (HDMS) and air dried. All specimens were mounted on aluminium stubs using double-sided carbon tape and then were sputter coated with 15 nm gold in a sputter coater (Quorum

Technologies, Laughton, East Sussex, UK) and observed under a Zeiss Sigma 300 Field-Emission scanning electron microscope (ZEISS). Materials are listed in **Table 13**.

Scanning Electron Microscopy (SEM)		
Component	Manufacturer	Cat.No.
Glutaraldehyde	Electron Microscopy Sciences	16220
Sodium Cacodylate Tryhidrate	Electron Microscopy Sciences	12310
Poly-L-Lysine	Merck Millipore	A-005-C
HMDS	Sigma	440191

Table 12. Listed materials applied for SEM.

7.9. Fluorescent microscopy and reverse swelling assay

Apical-in and apical-out organoids were attached to poly-L-lysine coated cover glasses and were incubated in HEPES solution for 30 min at 37 °C with 5% CO_2. BCECF-AM, Fura2-AM (5-5 µmol/L), MQAE (2 µmol/L) and SBFI-AM (10µmol/L) fluorescent indicators were applied for pH, Ca^{2+}, Cl^- and Na^+ measurements, respectively as previously described [21]. After loading with the fluorescent indicator, the samples were mounted on an Olympus IX73 inverted microscope and were excited with a CoolLED PE-4000 (BCECF-AM) or a CoolLED pE-340fura (Fura2-AM, MQAE and SBFI-AM) illumination system. Filter combinations for each fluorescent dye were described previously [18,21]. Hamamatsu Orca-Flash 4.0 sCMOS camera and 20X water immersion objective (Olympus; NA: 0.8) with a temporal resolution of 1 sec were used for capturing fluorescent signals. Ratiometric image analysis for pH_i measurements was performed by Olympus Excellence software. Fluorescence signals of Fura2- and MQAE-loaded samples were normalized and represented as F1/F0 values. During reverse swelling assay transmission light illumination was applied. Images were taken in every minute and were analyzed and quantified by ImageJ software. Reagents and inhibitors applied in experiments are listed in **Table 13-14**.

Fluorescent microscopy and reverse swelling assay						
		Applied solutions				
Component	Manufacturee Cat.No.	Standard HEPES pH=7.5	Ca^{2+} free HEPES pH=7.5	Standard HCO_3^-	Cl^- free HCO_3^-	Na^+ free HEPES pH=7.5
NaCl	Sigma, S9888	140 mM	142 mM	115 mM	-	-
KCl	Sigma, P3911	5 mM	5 mM	5 mM	-	5 mM
$MgCl_2$	Sigma, M2670	1 mM	1 mM	1 mM	-	1 mM
$CaCl_2$	Sigma, 223506	1 mM	-	1 mM	-	1 mM
HEPES	Sigma, H3375	10 mM	10 mM	-	-	10 mM
Glucose	Sigma, G8270	10 mM	10 mM	10 mM	10 mM	10 mM
$NaHCO_3^-$	Sigma, S6014	-	-	25 mM	25 mM	
EGTA	Sigma, E4378	-	1 mM	-	-	
Na-gluconate	Sigma, S2054	-	-	-	115 mM	
K_2SO_4	Sigma, P9458	-	-	-	2.5 mM	
Mg-gluconate	Sigma, M7554	-	-	-	1 mM	
Ca-gluconate	Sigma, C8231	-	-	-	6 mM	
N-Methyl-D-glucamine	Sigma, M2004-500G	-	-	-	-	140 mM

Table 13. Listed components of all applied solutions.

Fluorescent microscopy and reverse swelling assay		
Component	Manufacturer	Cat.No.
Poly-L-lysine	Sigma	P8920-100ML
Cover glass	VWR	ECN 631-1583
Fura2-AM	Invitrogen	F1201
MQAE	Invitrogen	E3101
BCECF, AM	Biotium	51012
SBFI, AM	Invitrogen	S1263
CPA	Tocris	1235
GSK7975A	Sigma	5.34351
Forskolin	Tocris	1099
CFTRinh-172	Biotechne	3430
VX-770	Merck Millipore	530541

Table 13. Listed further materials for fluorescent microscopy and reverse swelling assay

7.10. Statistical analysis

Data are expressed as means ± SEM. Significant difference between groups was determined by Mann-Whitney test. $P < 0.05$ was accepted as being significant. All statistical analysis were carried out by GraphPad Prism software (Version 8.3.1.).

8. RESULTS

8.1. Primary epithelial organoids established from human pancreatic tissue samples by enzymatic digestion retain ductal characteristics and polarity.

Pancreatic tissue samples were collected from 11 cadaver donors with no documented exocrine or endocrine pancreatic disease (6 male and 5 female patients; mean age 48±9.798 years; mean BMI 25.72 kg/m^2). After mechanical dissociation and enzymatic tissue digestion human pancreatic organoid cultures (hPOCs) were established in ECM (Matrigel) and grown in organoid feeding media containing Wnt3A/R-spondin/Noggin. Conventional organoids with apical-in polarity were successfully generated from all 11 samples, which were subcultured and cryopreserved in large quantities after the first passaging step for further applications such as creating polarity switched apical-out hPOCs (**Figure 4.**).

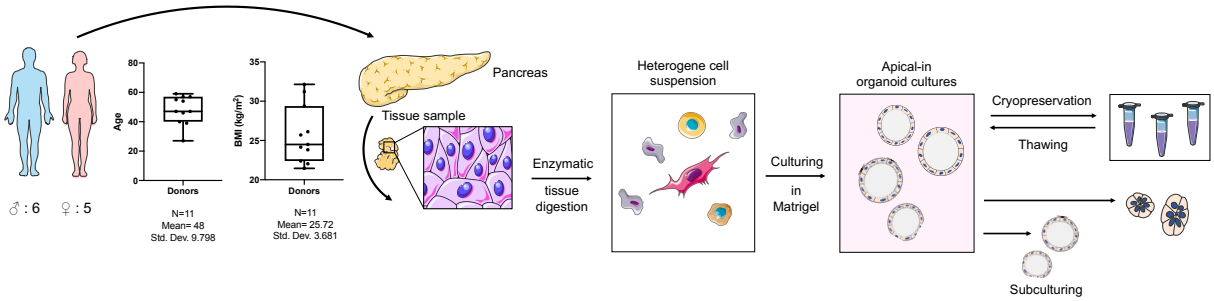

Figure 4. Schematic overview of sample processing from sample collection to apical-out organoid generation and basic characteristics of the cadaver donors (N=11, mean age: 48±9.798 years and mean BMI: 25.72±3.681 kg/m^2).

Cystic organoids appeared in the heterogeneous cell suspension on the second day of culture, while erythrocytes, acinar and stromal cells degraded. During passaging the organoids were enzymatically digested to single cells ensuring the clonal growth of the hPOCs (**Figure 5.**). Based on this, we can conclude with high confidence that manual isolation of human pancreatic ductal fragments is not necessary to generate organoids, and with the current method we describe, the initial organoid number does not depend on the number of ductal fragments, representing a more efficient methodology. Since we established OCs from a heterogeneous cell culture after tissue digestion, we were also interested to see whether the culture would become highly homogenous in terms of cell composition by inducing only epithelial cell division and whether a pure epithelial cell culture could be achieved. To this purpose, RNA was isolated from grown human organoid cultures (5 biological replicates) and transcriptome analysis was performed to investigate the composition of the cell culture by examining cell fate and gene expression patterns specific to different cell types of the pancreas.

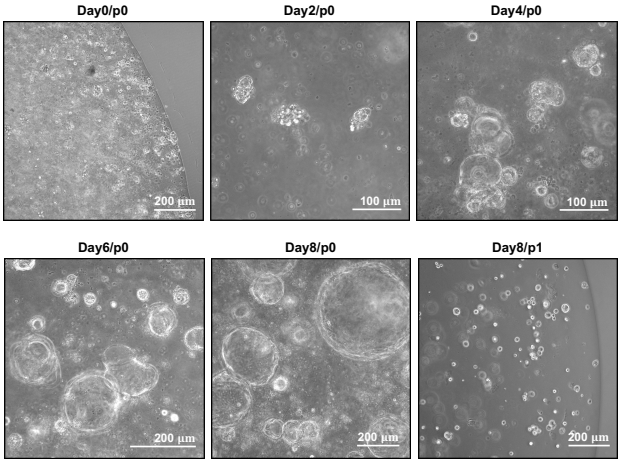

Figure 5. Transmitted light images demonstrate growth of human pancreatic organoids from the time of isolation (Day0/passage0) to first passage (Day8/p1).

RNA-sequencing showed the active expression of the adult stem cell marker *LGR5* (Leucin-rich repeat-containing G-protein coupled receptor 5) and ductal markers such as cystic fibrosis transmembrane conductance regulator (*CFTR)*, cytokeratin 19 (*KRT19)*, occludin (OCLN), SRY-Box transcription factor 9 (*SOX9*), epithelial cell adhesion molecule (*EPCAM*), e-cadherin (*CDH1*), Hes family BHLH Transcription Factor 1 *(HES1*) was observed, while the absence of acinar- (amylase, *AMY1A-C*) endocrine- (Pancreatic polypeptide, *PPY;* Insulin, INS; Chromogranin A-B, (*CHGA-B*) and hematopoietic (vascular endothelial cadherin, C*DH5*) markers confirmed that the human pancreatic organoids containing ductal epithelial cells exclusively (**Figure 6.**).

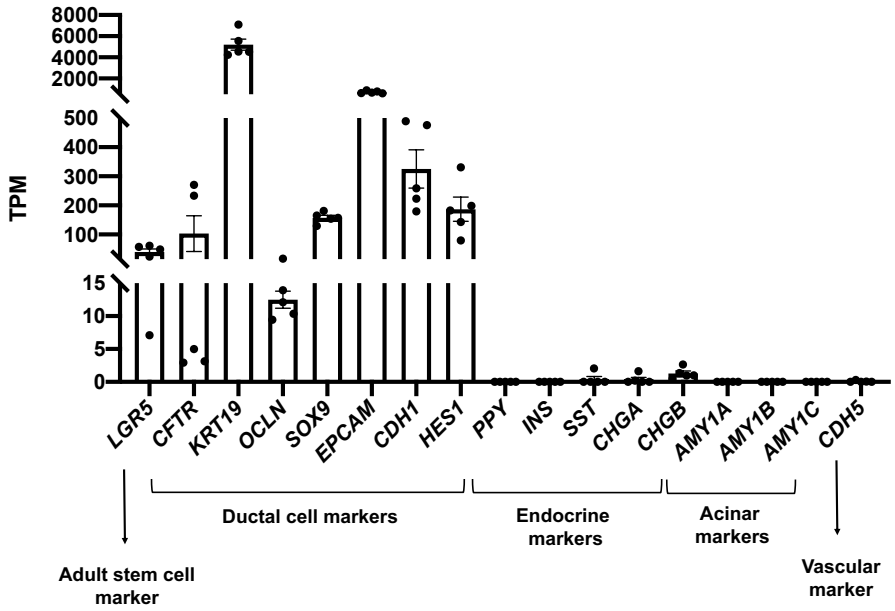

Figure 6. Transcriptome analysis of human pancreatic organoid cultures (hPOCs) by RNA-sequencing (N=5). Data are indicated in TPM value (Transcript/million).

Next, we also confirmed the expression and localization pattern of the key ductal markers on the protein level. These ductal markers such as SOX9, HNF1B and FOXA2 showed a typical nuclear localization pattern, whereas KRT19 displayed intracellular reticular expression, which is typical for a cytoskeletal protein. Moreover, the apical-to-basal polarity of the organoids was evidenced by the apical membrane localization of CFTR and OCLN and the basolateral expression of NBCe-1 (**Figure 7.**).

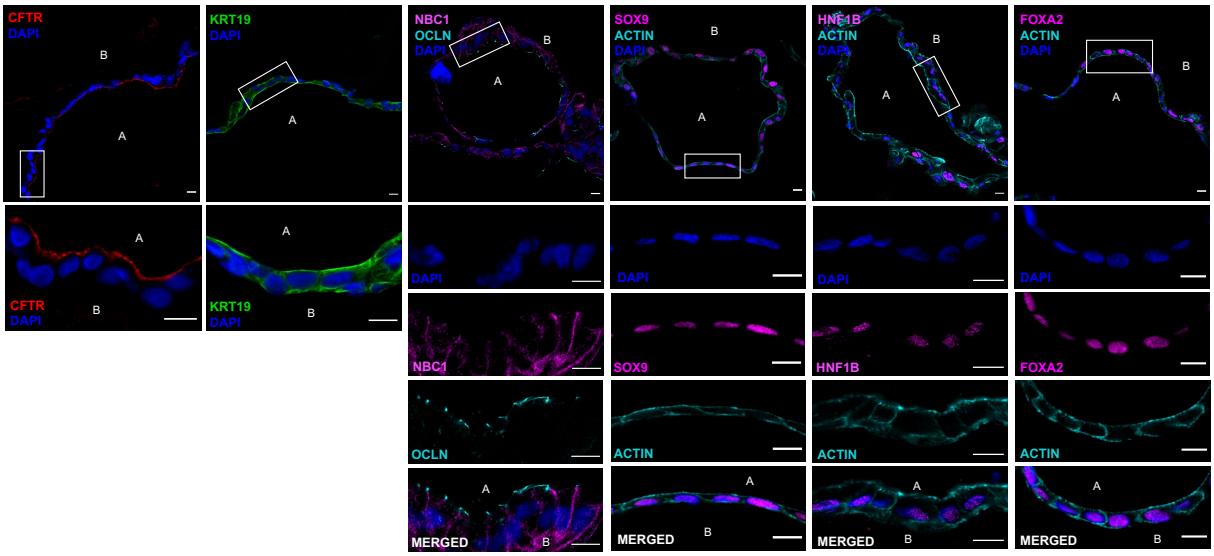

Figure 7. Confocal images demonstrate the localization CFTR, KRT19, NBC1, OCLN, SOX9, ACTIN, HNF1B and FOXA2 in apical-in human pancreatic organoids (scale bar: 10 µm; A: apical side; B: basolateral side).

8.2. Extracellular matrix removal induces a polarity switch that reduces the epithelial cell tension in pancreatic organoids

Previously, Co et al. successfully controlled the polarity of colon organoids by removal of the extracellular matrix scaffold [29,30], which resulted in a polarity switch of the cells. The apical-out organoids maintained the barrier function allowing the study of host-pathogen interactions. Notably, the epithelial cell functions, such as ion and fluid secretion were not assessed in those manuscripts. To induce a polarity switch in human pancreatic organoids first we generated apical-in organoids in ECM, which then were placed into a suspension culture. We observed that after 48 h the morphology of the organoids was changed and the typical cystic form was replaced by a denser structure formed by a columnar cell layer (**Figure 5.A.**). Immunofluorescence staining of the apical CFTR, ACTIN and OCLN revealed that the morphological changes were also followed by the redistribution of intracellular proteins (**Figure 5.A. and B.**).

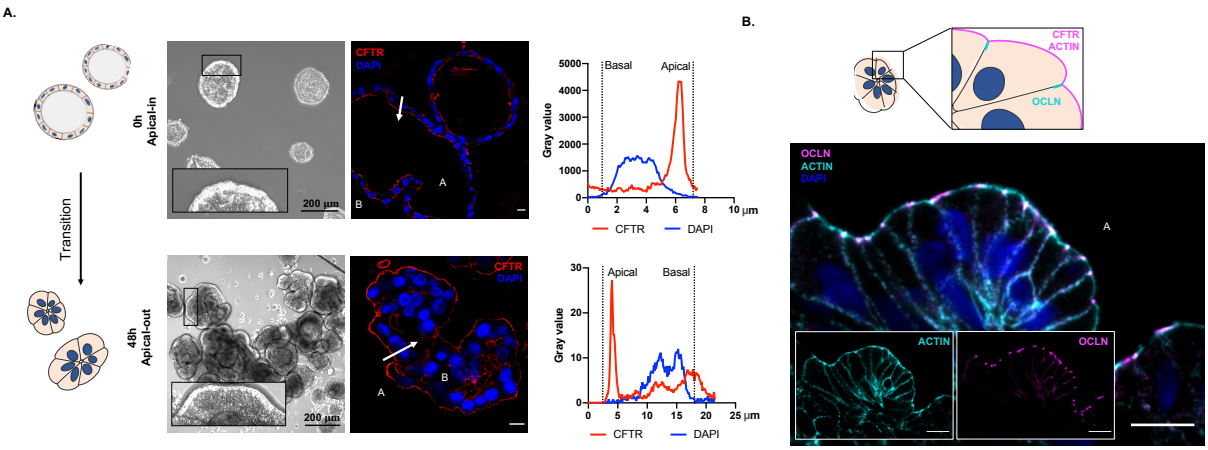

Figure 8. A. Schematic drawing and transmitted light images demonstrate the 48-hour-long transition (polarity switch) in suspension culture. The change of CFTR localization is presented by confocal images and line profile analysis of cross sectioned apical-in and apical-out hPOCs (scale bar: 10 µm; A: apical side; B: basolateral side, white arrow represents the axis of the line profile analysis). **B.** The polarity switch was further confirmed by immunofluorescent labelling of Occludin (OCLN) and ACTIN filaments at the apical side (outer side) of the apical-out hPOCs.

Previously we demonstrated the presence of brush border on the luminal membrane of mouse pancreatic organoids (**Figure 2.**), which can promote epithelial secretion by increasing the membrane surface [21]. To further decipher the effect of ECM removal on the organoids, we determined the expression of genes participating in microvillus formation and maintenance [51,52].

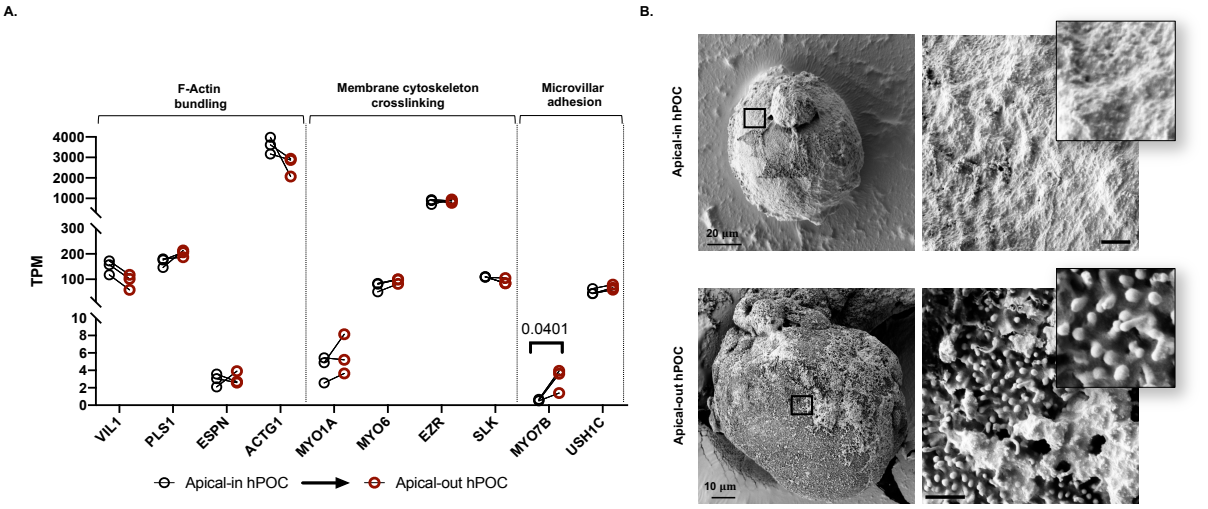

Figure 9. A. Transcriptomic comparison of genes responsible for the formation and organization of microvilli in apical-in and polarity switched apical-out hPOCs. Data are indicated in TPM value (Transcript/million). Genes are classified into the following groups based on the function of their protein product: genes responsible for F-actin bundling, membrane cytoskeleton crosslinking and intermicrovillar adhesion. **B.** Scanning Electron Microscopy (SEM) pictures of hPOCs revealed brush border and microvilli formation on the outer surface of the apical-out organoids which was not observed on conventional apical-in organoids (scale bars on enlarged images represent 1 µm).

Our results showed that there were no significant differences in the expression of genes involved in F-actin bundling, membrane cytoskeleton crosslinking or intermicrovillar adhesion upon polarity switching (**Figure 9.A.**). However, the expression of myosin 7B was significantly higher in apical-out organoids. These transcriptomic data suggest that the polarity change may increase the formation of microvilli and the brush border. In addition, scanning electron microscopy revealed the formation of a dense brush border on the outer surface of the polarity-switched human pancreatic organoids (**Figure 9.B.**).

The apical-in organoids display vectorial ion and fluid secretion into the lumen [21,53] resulting in an elevated intraluminal pressure and cyst formation, which may also affect the cell shape. Therefore, we examined the size of the organoids before (in ECM) and after (in suspension) the polarity change. We found that the diameter of the organoids significantly decreased, whereas the cell density increased after the polarity switch (**Figure 10.A.**). Next, we compared the diameter of cells and nuclei in the apical-in and apical-out hPOCs, which revealed that the longitudinal diameter of the cells and nuclei significantly reduced in apical-out organoids leading to the formation of a columnal epithelial cell layer (**Figure 10.B.**).

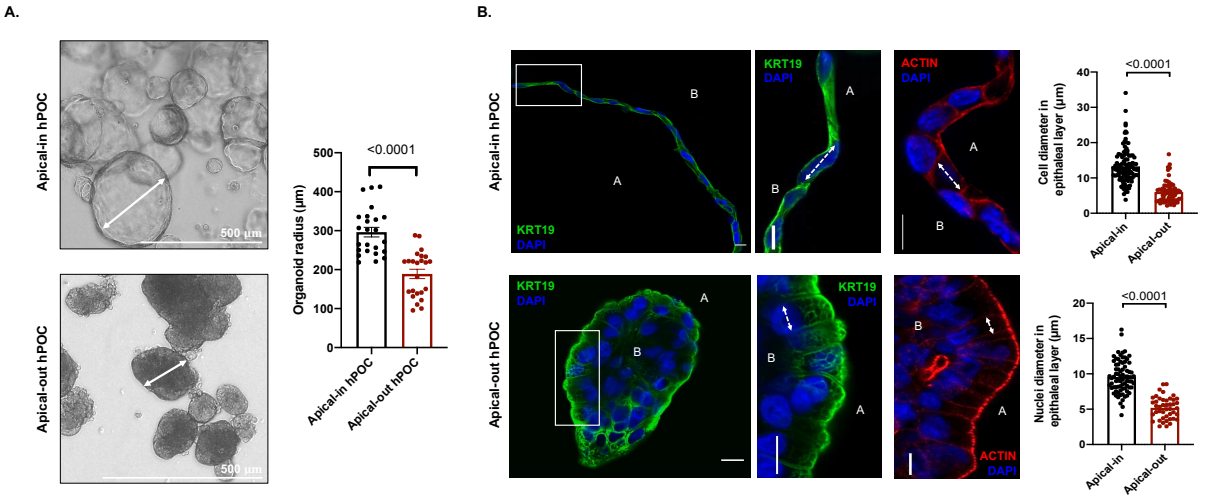

Figure 10. Phase contrast images and statistical comparison of the significant diameter difference between apical-in (growing in ECM) and apical-out (suspension culture) hPOCs. **F.** Confocal images of crossed sectioned organoids and bar charts demonstrate the significant difference in diameter of cells and nuclei between apical-in or apical-out hPOCs (scale bar: 10 µm; A: apical side; B: basolateral side; white arrows demonstrate the diameter of cells or nuclei).

In epithelial cells, PIEZO1 function as a mechanosensor mediating extracellular Ca^{2+} influx upon increased intraluminal tension [28]. Our results also showed that hPOCs express *PIEZO1* (**Figure 11.A-B.**) that can participate in the regulation of epithelial ion and fluid secretion. Finally, we showed that the polarity switching decreases the gene expression of cyclins, which are major elements of cell division, suggesting a decrease in the cell proliferation. Our results

highlight that the removal of the ECM can induce a polarity switch in the hPOCs that eliminates the intraluminal pressure leading to a columnar cell morphology, which can be observed in primary ductal cells in their physiological environment [21].

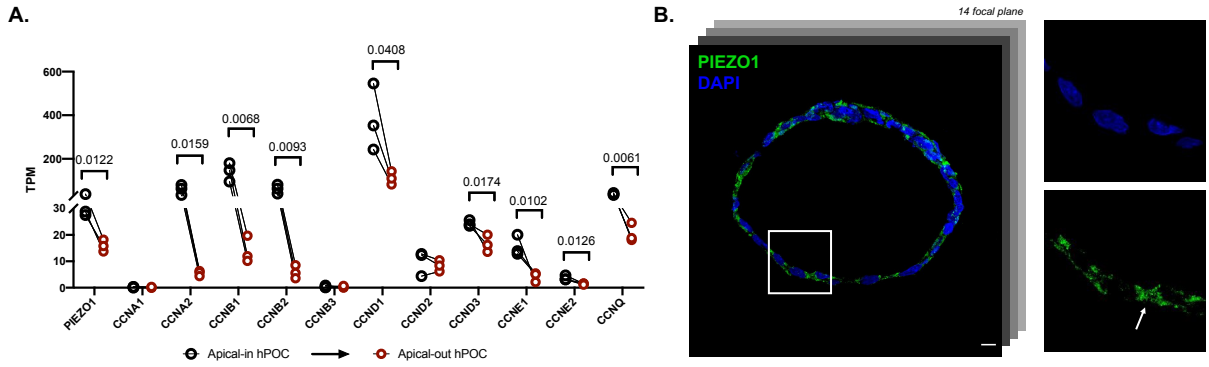

Figure 11. A. Comparative transcriptome analysis of apical-in (N=3) and apical-out (N=3) human pancreatic organoid cultures by RNA sequencing. Data are indicated in TPM value (Transcript/million). **B.** Merged confocal (Z-stack) picture demonstrates the presence of PIEZO1 protein on Apical-in hPOCs. The highlighted detail and the arrow show the localization of PIEZO1 mainly between the elongated cells (scale bar: 10 µm).

8.3. The resting intracellular Ca^{2+} concentration is more consistent in apical-out hPOCs

Ca^{2+} signaling is one of the major signal transduction pathways regulating secretory processes in the exocrine pancreas whereas in pathophysiological conditions, inflammatory processes are always characterized by disturbed Ca^{2+} homeostasis [6,54]. Since the above-described intraluminal tension in the apical-in culture may influence the epithelial Ca^{2+} homeostasis via PIEZO1 activation, we compared the Ca^{2+} signaling in apical-in and apical-out hPOCs.

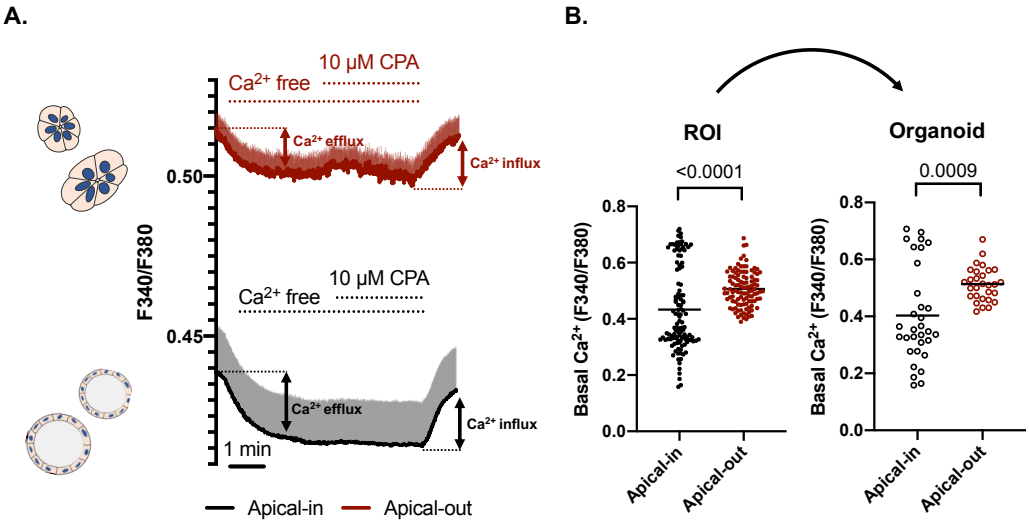

Figure 12. A. Average traces demonstrate the resting Fura2-AM ratio. Removal of the extracellular Ca^{2+} triggered a drop of intracellular Ca^{2+} presumably due to cytosolic Ca^{2+} efflux. 10 µM CPA (cyclopiazonic acid) was administrated in Ca^{2+} free HEPES for ER Ca^{2+} depletion,

whereas re-addition of the extracellular Ca^{2+} initiated store operated Ca^{2+} entry (SOCE). **B.** Bar charts show the significant difference in basal Ca^{2+} levels between apical-in and apical-out organoids based on the investigated ROIs which was also converted into individual organoids. Evaluation of the resting intracellular Ca^{2+} levels revealed a significantly elevated basal Ca^{2+} level in apical-out hPOCs compared to apical-in organoids **(Figure 12.A-B.)**. On one organoid multiple ROIs were selected during the measurement. To translate the signals detected in ROIs on organoid level, all ROIs selected on an individual organoid were pooled and plotted. In both cases the basal intracellular Ca^{2+} levels were significantly higher in the apical-out organoids **(Figure 12.A.)**. Interestingly, if each organoid was plotted separately with the mean value of all ROIs, it is clearly shown that apical-in organoids have 2.8 times higher basal Ca^{2+} level deviation than their apical-in counterparts **(Figure 13.)**.

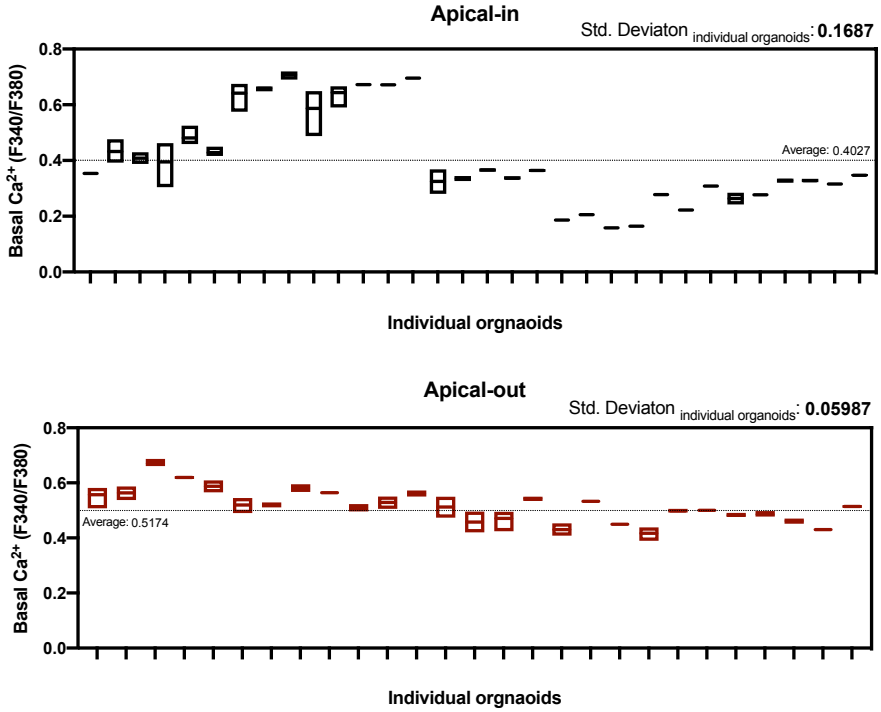

Figure 13. Graphs demonstrate the standard deviation of basal Ca^{2+} levels in individual organoids from the mean value in apical-in and apical-out human pancreatic ductal organoids.

These observations suggest that the resting intracellular Ca^{2+} is more constant in the apical-out hPOCs. Notably, no significant difference was found in either the Ca^{2+} efflux or Ca^{2+} influx rates in a similar evaluation process **(Figure 3.D-E.)**, suggesting that the observed deviation in the basal intracellular Ca^{2+} in the apical-in organoids may be a result of a pre-stimulated state (such as the activation of PIEZO1 by mechanical stress), which varies among different organoids.

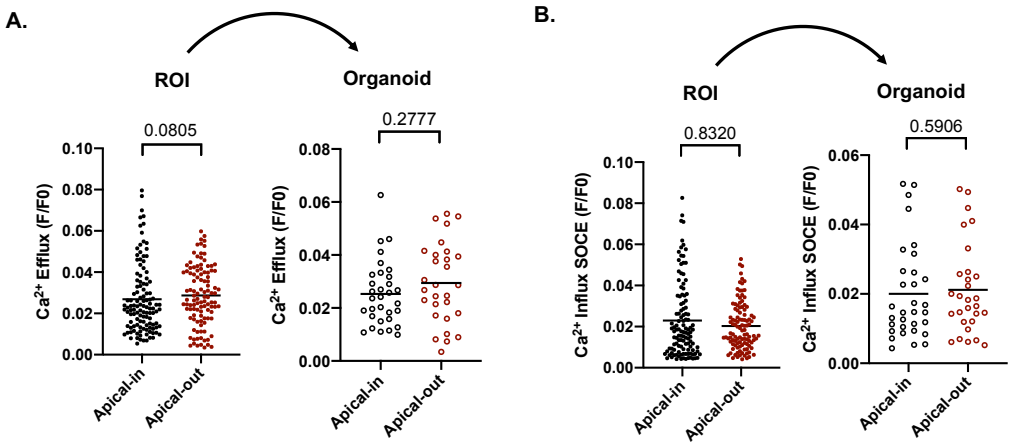

Figure 14. Bar charts show maximum change in Ca^{2+} levels during Ca^{2+} efflux (**A.**) and CRAC channel activity (**B.**) (Ca^{2+} influx) with no significant differences in apical-in and apical-out hPOCs.

Since it was previously shown that ORAI1 CRAC channel is a promising therapeutic target to prevent epithelial cell Ca^{2+} overload we also investigated the channel localization in apical-out hPOCs which retained its apical membrane expression **(Figure 15.)** [18].

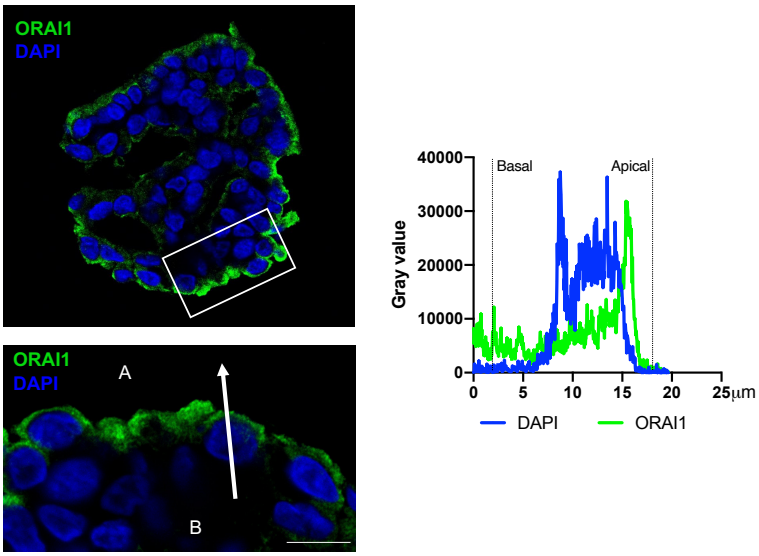

Figure 15. Confocal images and line profile analysis demonstrate the apical localization of ORAI1 on cross sectioned apical-out hPOCs (scale bar: 10 µm; A: apical side; B: basolateral side, white arrow represents the axis of the line profile analysis).

To rule out that the changes observed in the intracellular Ca^{2+} homeostasis were caused by the altered expression of proteins involved in the Ca^{2+} signaling, we analyzed and compared the expression of several genes (**Figure 16.**). However no biologically meaningful changes were observed between apical-in and apical-out organoids. Taken together, our data suggest that resting intracellular Ca^{2+} level is more consistent in the apical-out hPOCs, which may be explained by the elimination of the intraluminal pressure and no pre-stimulation in this culture.

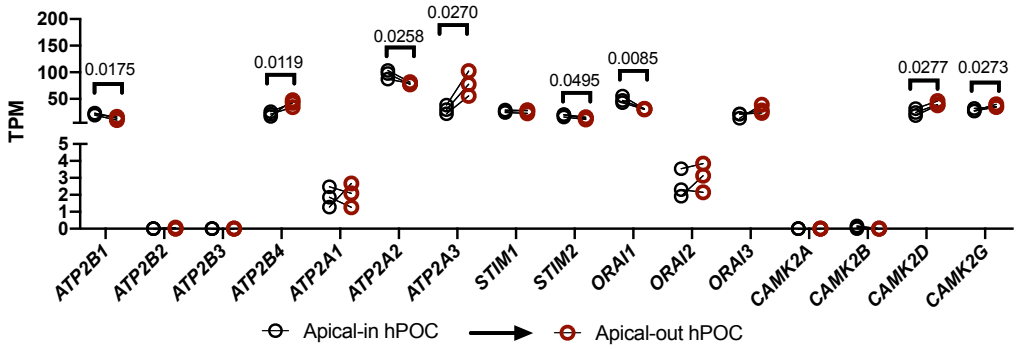

Figure 16. Comparative (apical-in/apical-out) transcriptomic analysis of major genes responsible for Ca^{2+} handling. Data are indicated in TPM value (Transcript/million).

8.4. Functionally active Anoctamin 1 and ENaC are expressed in human pancreatic ductal cells

Pancreatic organoids enabled the direct study of the human pancreatic secretory functions. According to the currently accepted model CFTR plays a central role in the human pancreatic ductal Cl^-/HCO_3^- secretion, whereas other Cl^- channels, such as Ca^{2+} activated Cl^- channels (CaCC) are not expressed in the ductal cells, or have marginal role [55–58]. In contrast in other species, such as rodents, CaCC are important in the pancreatic ion secretion [59]. These early pharmacological studies were also confirmed by RNA-sequencing, which revealed that *Ano1* is the dominantly expressed CaCC channel in apical-in mouse pancreatic organoids **(Figure 16.A.)**, which is 45.73 times higher than *Cftr* **(Figure 16.B.)**.

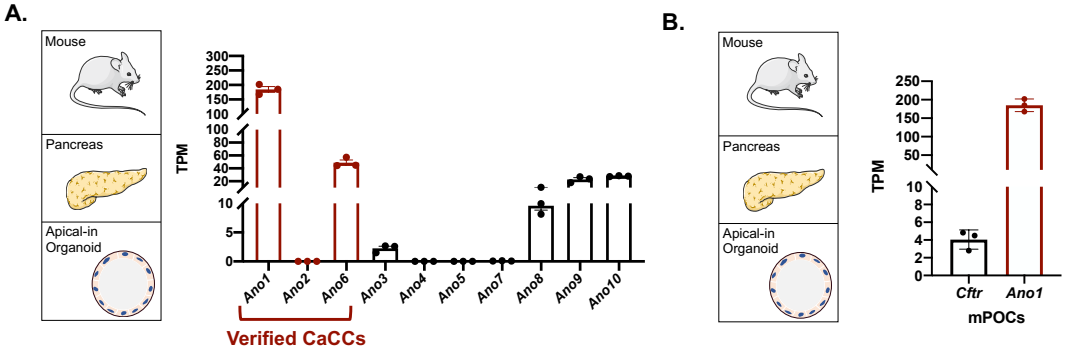

Figure 16. A. Bar charts demonstrate RNA-seq profile of ANO family members in mouse (N=3) pancreas derived organoid cultures (mPOCs). Gene expression profile of *CFTR and ANO1* determined in mouse (**B.**) (N=3) pancreatic organoids.

To gain human relevant information, we also analyzed the expression of the anoctamins (ANO) and the epithelial sodium channel (ENaC) subunits, which was not found previously in the pancreatic ductal cells [42], in human pancreatic organoids. Interestingly, transcriptome analyses revealed a relatively high expression of *ANO1* and *SCNN1A* in the apical-in human pancreatic organoids **(Figure 17.)**.

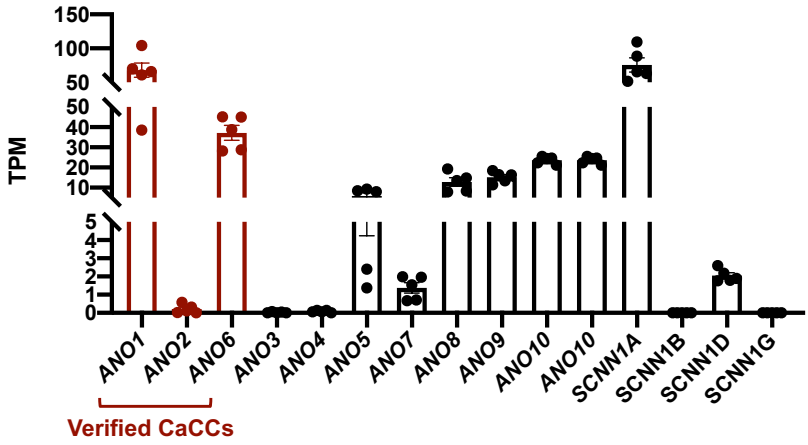

Figure 17. Gene expression profile of *ANO* family members and *SCNN1A/B/D/* in apical-in hPOCs. Data are indicated in TPM value (Transcript/million).

The average expression of *CFTR* and *ANO1* in the human pancreatic organoids is nearly identical suggesting that ANO1 as the dominantly expressed ANO family member may contribute to the ion secretion in human ductal cells **Figure 18.)**.

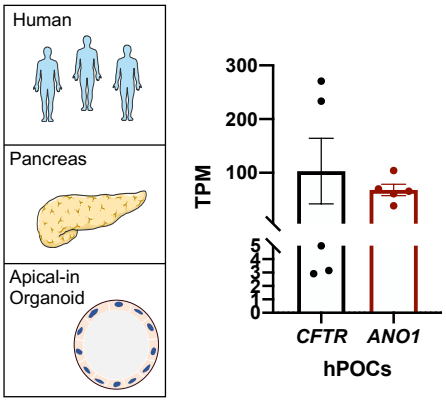

Figure 18. Bar charts demonstrate RNA-seq profile of ANO family members in human (N=5) pancreas derived organoid cultures (hPOCs)

To confirm these findings in human pancreatic tissue, we next demonstrated the expression of ANO1 and ENaC by immunohistochemistry carried out on human pancreas tissue section and by immunofluorescent labelling performed on apical-out hPOCs **(Figure 19.A.)**. The observed pattern suggests that also ANO1 and ENaC are dominantly present in the apical membrane of the ductal epithelial cells. When we assessed the effect of the polarity switch on the gene expressions, we observed that *CFTR* is not affected by this process, while the expression of *ANO1* was significantly decreased suggesting its stronger dependence on intraluminal pressure **(Figure 19.B.)**.

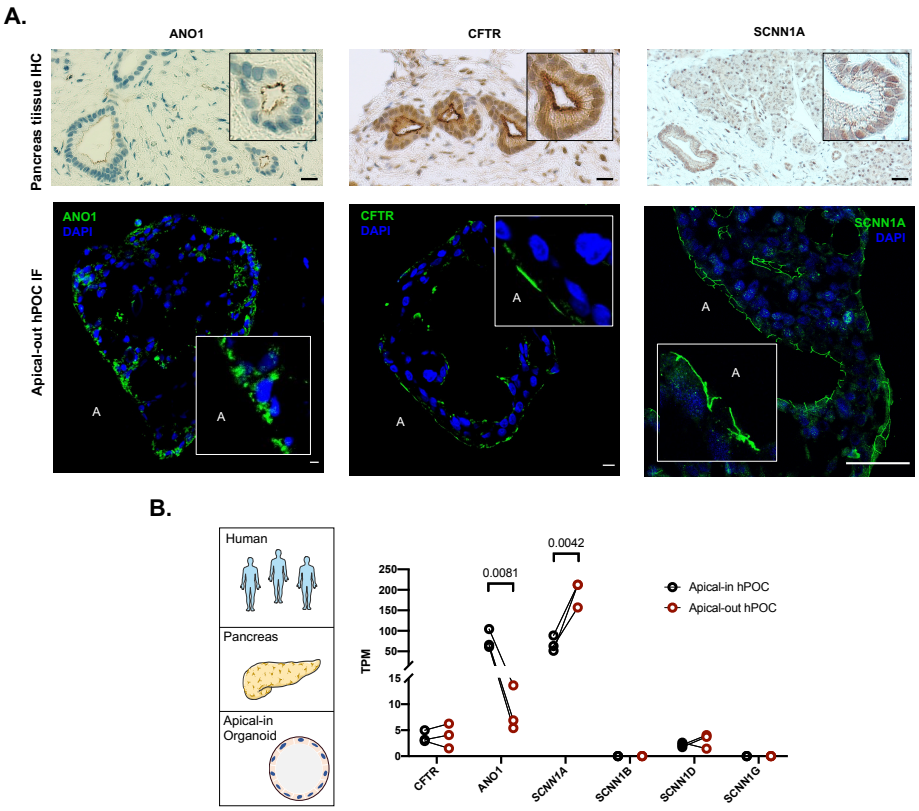

Figure 19. A. Comparison of IHC performed on sectioned pancreatic tissue and IF-labeled apical-out hPOC to demonstrate retained apical localization of ANO1, CFTR and SCNN1A (scale bar: 10 µm; A: apical side). **B.** Transcriptomic comparison of CFTR, ANO1, SCNN1A/B/D/G in in apical-in and polarity switched apical-out hPOCs (N=3). All data are indicated in TPM values (Transcript/million).

Next, we used an intracellular Cl^- concentration ($[Cl^-]_i$) sensitive fluorescent indicator, MQAE to follow ANO1 driven Cl^- extrusion. Due to the chemical characteristics of MQAE, the emitted fluorescent signal inversely correlates with $[Cl^-]_i$. Apical-out hPOCs were challenged with 10 µM T16inhAO1, a pharmacological inhibitor of ANO1, for 5 min before the extracellular Cl^- removal from the HCO_3^-/CO_2-buffered solution.

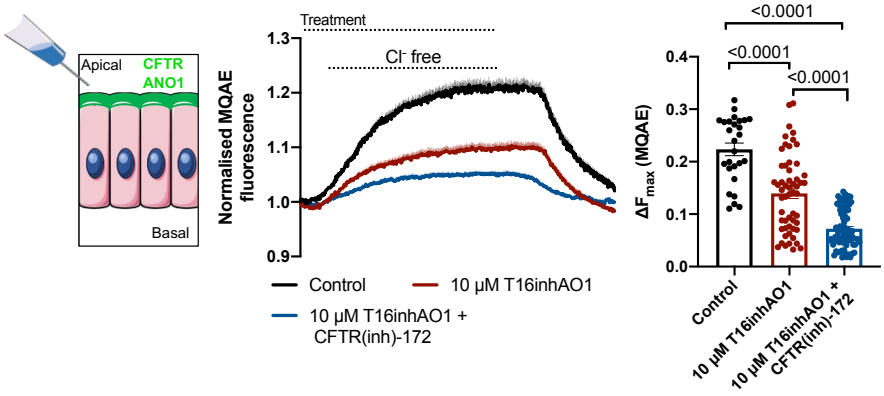

Figure 20. Average traces and bar charts demonstrate the intracellular Cl^- level measurements performed by MQAE in apical-out organoids. The intracellular $[Cl^-]_i$ and the intensity of

fluorescence are inversely proportional. Challenging apical-out organoids with Cl^- free extracellular solution resulted in a decrease in $[Cl^-]_i$ which was significantly reduced by 10 µM of ANO1 inhibitor (T16inhAO1) while in combination with 10 µM CFTR(inh)-172 the mean maximum response was almost completely abolished.

These experiments revealed that 10 µM T16inhAO1 significantly reduced the intracellular Cl^- extrusion. Moreover in combination with 10 µM CFTR(inh)-172 the maximum response was further reduced **(Figure 20.)**. Direct application of siRNA to knock down gene expressions in organoids is hindered by the presence of Matrigel, which limits the cell permeation of siRNAs **(Figure 21.).**

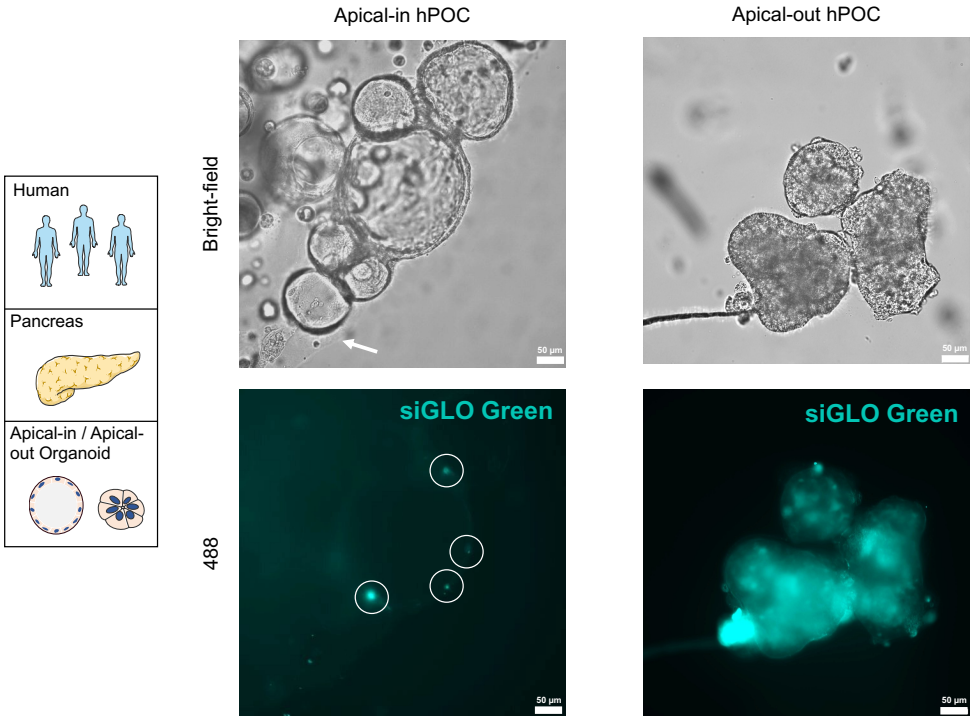

Figure 21. Transfection control (siGLO Green) assay of apical-in organoids growing in ECM (Matrigel) and apical-out organoids maintained in suspension. The white arrow in the brightfield image marks the border of the Matrigel, while the white circles show the rarely transfected cells that were able to take up siGLO Green indicator. Apical out organoids kept in suspension were perfectly able to take up the transfection indicator.

However, this bottleneck was eliminated by culturing the organoids in suspension, which allowed the knock down of CFTR and ANO1 expression in apical-out organoids as verified by qRT-PCR, immunofluorescence staining and intensity profile analysis of the target proteins **(Figure 22.)**.

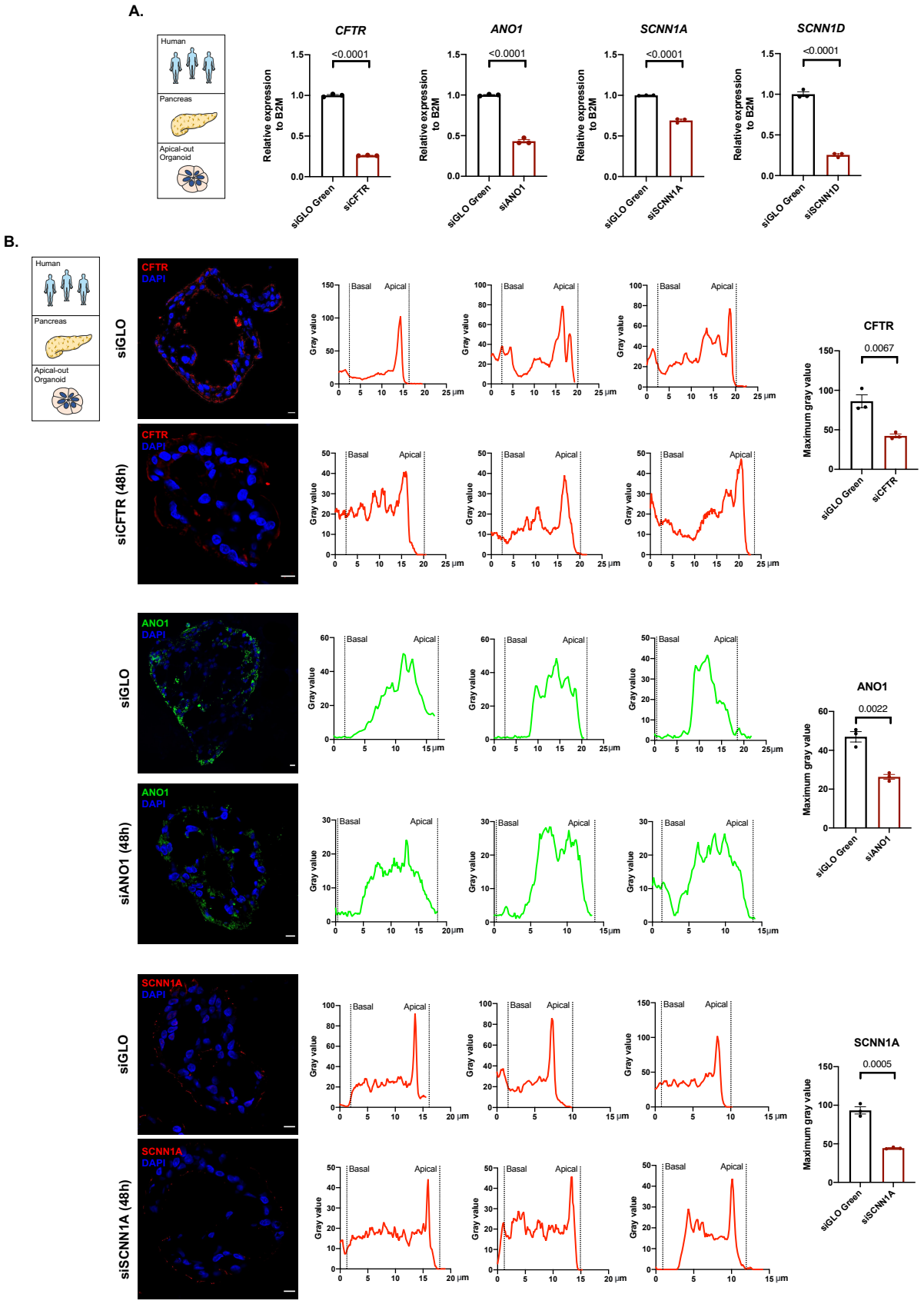

Figure 22. Validation of the 48-hour-long gene silencing method carried out on apical-out organoids. The efficiency of the pre-validated siRNA pools on the target genes' expression was verified at the level of mRNA by qRT-PCR (**A.**) and also at protein level by immunofluorescent

labelling (**B.**). All qRT-PCR raw data was analyzed by the ΔΔCq method, while in case of IF confocal pictures, data for three individual intensity profiles were collected from three distinct membrane areas and maximum intensity values of the independent intensity profiles are plotted on bar charts (scale bar: 10 µm).

Gene silencing experiments demonstrated that both siCFTR and siANO1 significantly decreased the apical Cl^- extrusion, which was further impaired by the combination of the two siRNAs **(Figure 23.)**. These results provide evidence of the significant contribution of ANO1 to the Cl^- secretion of human pancreatic ductal cells, which may have a major and yet unrevealed physiological relevance.

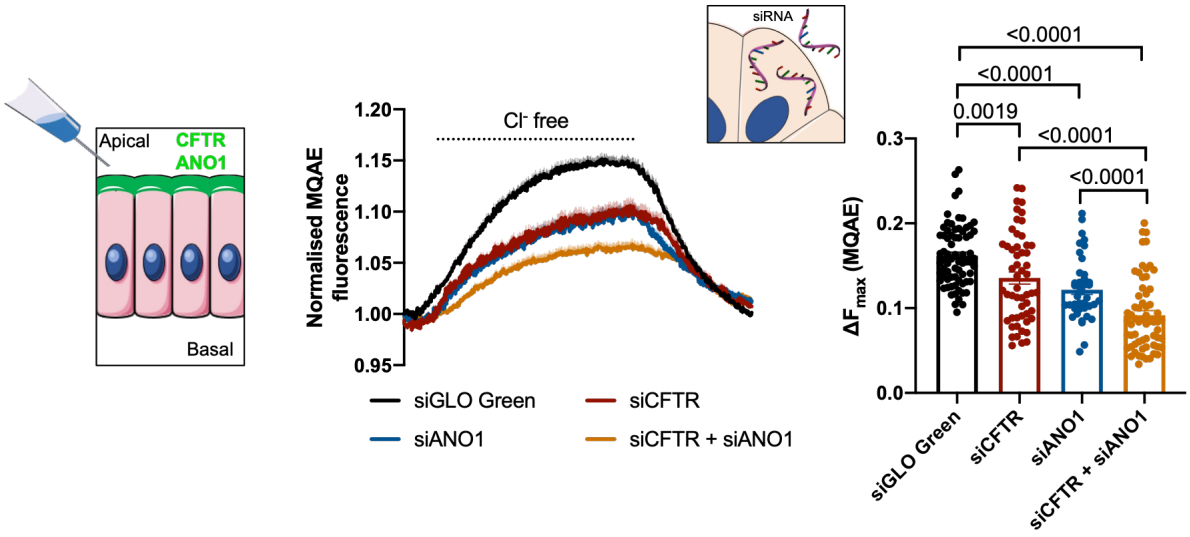

Figure 23. Average traces and bar charts demonstrate the result of siRNA transfection by 50 nM siGLO Green (control), si*CFTR*, or si*ANO1* in the same experimental setup. Both siRNAs, alone and in combination significantly reduced Cl^- efflux compared to the control.

ENaC is usually expressed on the apical plasma membrane of the epithelial cells and participates in Na^+ reabsorption [60,61]. ENaCs are heterotimers that are formed by α, β, and γ subunits (with a 1:1:1 stoichiometry) encoded by different genes (*SCNN1A, SCNN1B, SCNN1G*) [35,62]. Another subunit known as δ (*SCNN1D)* has been identified in humans [40]. It was previously shown that functional ENaC formed by single or only two subunits, exist in certain tissues but the exact structure and capacity of the channel in pancreatic ductal cells remained unexplored [63]. Interestingly, among 4 subunits, remarkable expression of *SCNN1A* and moderate expression of *SCNN1D* were detected in hPOCs **(Figure 17.)**. Moreover, the subunit α (SCNN1A) was detected in the apical membrane of polarity shifted hPOCs by immunofluorescent labelling **(Figure 19.A.)**. Next, siRNA interference was applied to assess the functional activity of the channel. After 48h incubation with siSCNN1A and siSCNN1D,

apical-out hPOCs were challenged with 100 µM amiloride from the apical membrane, which resulted in a rapid decrease of the fluorescent ratio suggesting an indirect influence of the ENaC activity on the apical Cl^-/HCO_3^- exchange **(Figure 24.)**.

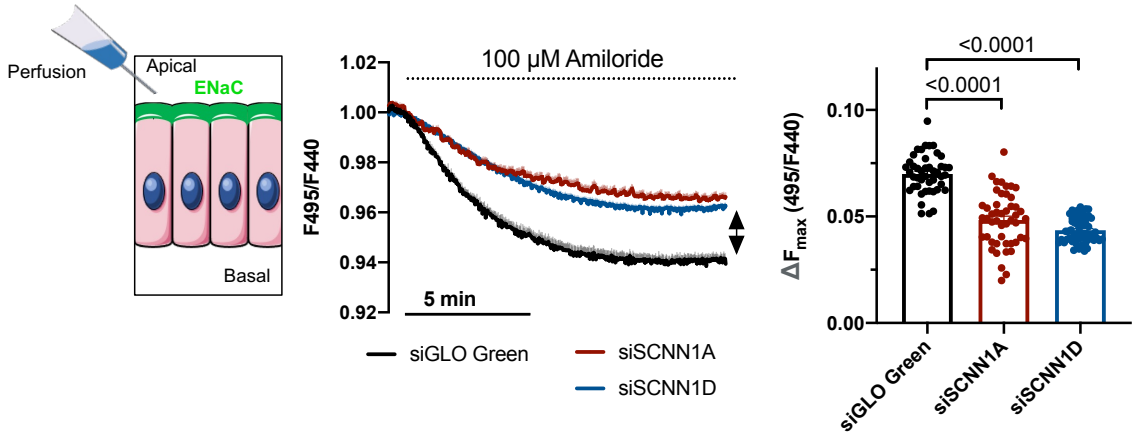

Figure 24. Average traces and bar charts demonstrate a significant difference in (BCECF-AM) fluorescent ratio between siGLO Green (control) and si*SCNN1A* or si*SCNN1D* treated apical-out hPOs in response to 100 µM amiloride. Average traces of 3-4 experiments are demonstrated in each measurement.

Notably, to achieve the significant decrease of the maximal response, the knock down of each subunit was sufficient suggesting that both isoforms are needed for the formation of the active channel. Furthermore, the intracellular Na^+ indicator SBFI was used to directly measure the contribution of SCNN1A and SCNN1D to the channel activity, which further confirmed that both subunits are mandatory for the function of ENaC as both siRNA treatment resulted in significantly reduced Na^+ influx **(Figure 25.)** These results suggest that SCNN1A and SCNN1D subunits are necessary for the constitution of a functional ENaC proteins in human pancreatic ductal cells.

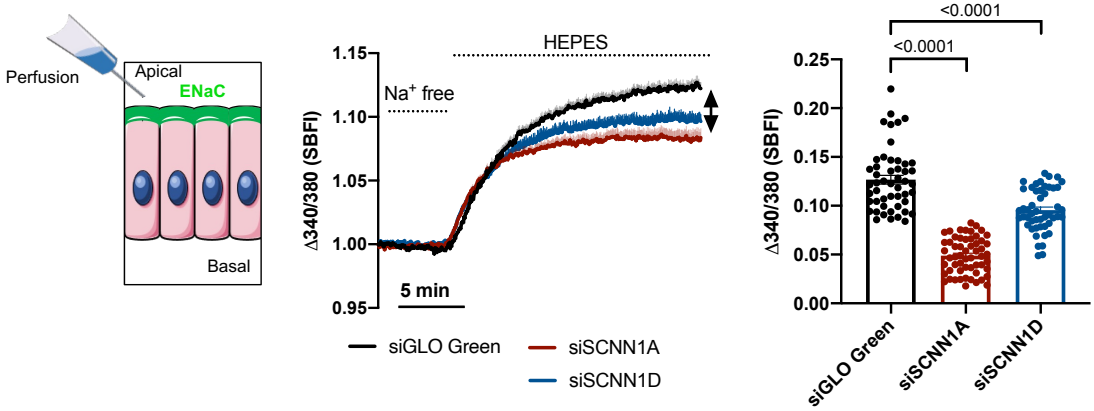

Figure 25. Average traces and bar charts demonstrate a significant difference in (SBFI) fluorescent ratio between the control and siRNA treated apical-out hPOs in response to Na^+ free solution Average traces of 3-4 experiments are demonstrated in each measurement.

8.5. Polarity switching improve the performance of organoids in available functional assays

To use of *ex vivo* models with translational relevance and improved throughput is currently an unmet need in pancreatic research. As an example, current drugs that are accepted for the treatment of cystic fibrosis have been designed to rescue the lung phenotype of CF, however the pancreatic phenotype have not been addressed yet. This is most likely due to the lack of access to functional human pancreatic cells. To assess CFTR activity in epithelial cells a widely used indirect functional assay is the forskolin-induced swelling (FIS) [64]. However, dynamic range of this technique is limited by the elevation of the intraluminal pressure within the organoids. By capitalizing the switched polarity of apical-out organoids, we performed reverse FIS assay to demonstrate the activity of the wild type CFTR. Under these experimental condition 10 µM forskolin (FSK) decreased the relative volume of the apical-out organoids, which was abolished by the administration of 10 µM CFTR(inh)-172 (**Figure 26.**) suggesting that this technique is suitable to measure the activity of the wild type CFTR as well.

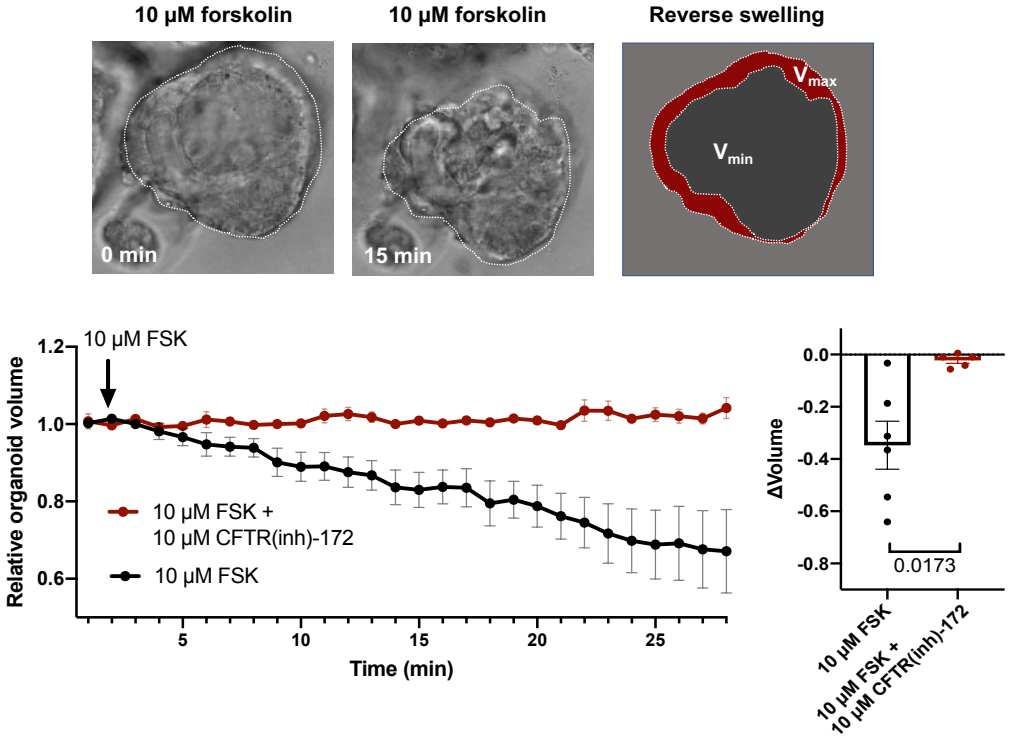

Figure 26. Transmitted light images and the relative organoid volume demonstrate the change of organoids during inverse swelling assay induced by 10 µM Forskolin (FSK). Relative change of organoid volume was normalized to baseline state. 10 µM CFTR(inh)-172 completely abolished the volume change.

Next, we wanted to compare further the performance of the apical-in and apical-out organoids in functional assays, therefore we assessed CFTR mediated Cl^- secretion by MQAE. The Cl^-

extrusion was significantly decreased by 10 µM CFTR(inh)-172 suggesting that the detected change is largely CFTR dependent in apical-in organoids **(Figure 27.A.)**.

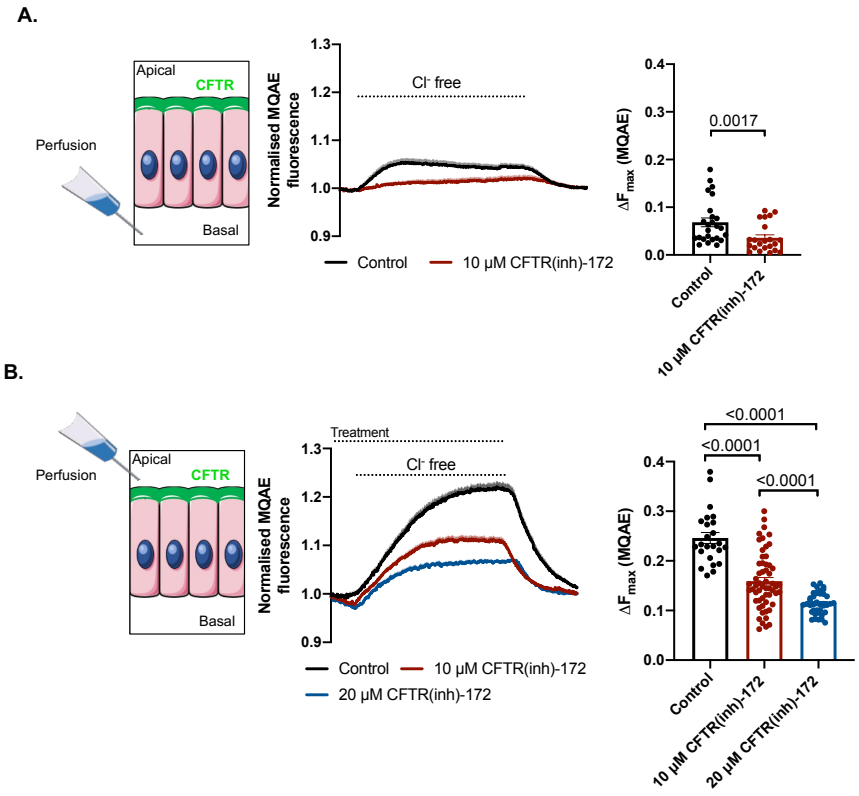

Figure 27. **A.** Intracellular Cl^- level was measured by MQAE in apical-in organoids. Challenging apical-in organoids with Cl^- free extracellular solution resulted in a decrease in $[Cl^-]_i$ which was abolished by 10 µM CFTR(inh)-172. Average traces of 3-4 experiments and bar charts demonstrate the significant difference between the investigated groups (control vs 10 µM CFTR(inh)-172). **B.** Elevated Cl^- extrusion observed in apical-out hPOs could not be completely abolished by 10 or 20 µM CFTR(inh)-172.

However, when the same protocol was applied on apical-out organoids, the response to Cl^- removal was higher than in conventional organoids presumably caused by the direct apical perfusion and lack of intraluminal pressure **(Figure 27.B. and Figure 28.)**.

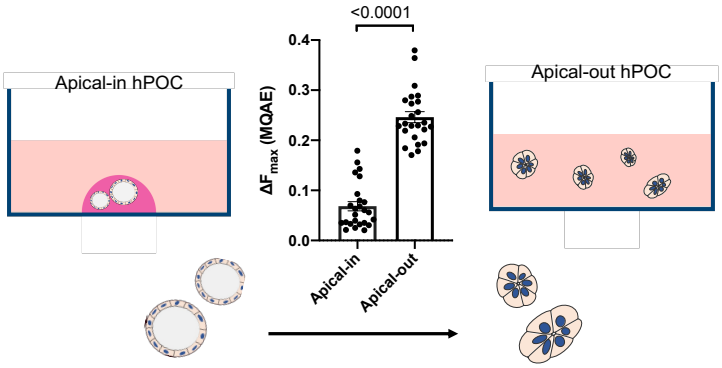

Figure 28. The bar chart demonstrates the comparison of detected maximum Cl^- extrusion of apical-in vs apical-out hPOCs.

Moreover, due to the enhanced resolution of the apical-out model, even the administration of a 20 µM CFTR(inh)-172 inhibitor could not completely abolish the Cl^- efflux process, confirming the involvement of additional channels, such as ANO1 **(Figure 27.B.)**. The direct access of the apical membrane also allowed to test the effect of a known CFTR potentiator, VX-770 on the CFTR activity on the pancreatic ductal cells. The administration of 10 µM VX-770 significantly enhanced Cl^- efflux in apical-out organoids and kept the steady-state at an elevated $[Cl^-]_i$ proving proof-of-concept evidence for the applicability of apical-out hPOCs in *in vitro* drug testing assays **(Figure 29.a-b.)**.

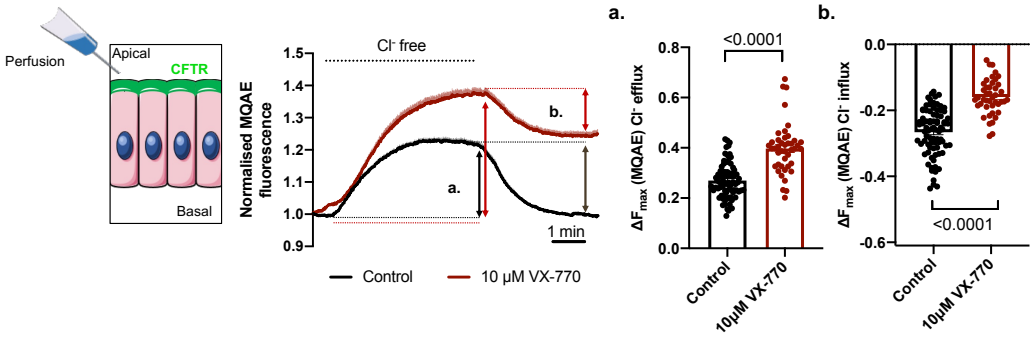

Figure 29. Average traces of 3-4 experiments and bar charts show the effect of the CFTR-potentiator VX-770 which significantly enhanced Cl^- efflux (**a.**) and which also established an elevated equilibrium in $[Cl^-]_i$ level upon reperfusion of the Cl^- containing solution (**b.**).

Finally, Cl^- and HCO_3^- exchanger (CBE) CBE activity was measured by using BCECF pH-sensitive dye with CFTR inhibition in HCO_3^-/CO_2 buffered solution. Cl^- withdrawal followed by direct apical perfusion of Cl^- containing HCO_3^- solution with simultaneous administration of 10 µM CFTR(inh)-172 decreased the slope of BCECF ratio (F495/F440) compared to the control group, which difference suggests indirect detection of CBE activity in hPOCs **(Figure 30.)**. These data suggest that apical-out hPOCs could provide significantly improved platform for *ex vivo* functional assays and pharmacological tests with increased throughput.

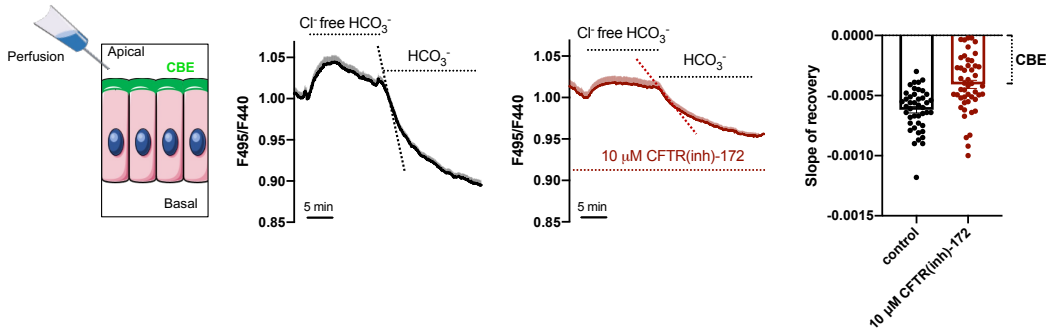

Figure 30. Intracellular pH was used for the detection of Cl^-/HCO_3^- exchanger (CBE) activity. Average traces and bar charts demonstrate the significant difference between slopes in control vs 10 µM CFTR(inh)-172 treated groups at post-withdrawal phase of the extracellular Cl^-. The difference between the mean slope values indicates CBE activity. Average traces of 3-4 experiments are demonstrated in each measurement.

9. DISCUSSION

We generated human pancreatic organoids and advanced the culture technique further by manipulating the polarity of the epithelial cells. By switching apical-to-basal polarity the elongated cell morphology observed in the apical-in organoids changed to a cuboidal shape in the apical-out cultures, which was accompanied by a more consistent resting intracellular Ca^{2+} level. Capitalizing the improved accessibility of the apical plasma membrane, we identified the expression and function of ANO1 and ENaC in the human ductal epithelial cells. Finally, we demonstrated that functional assays (such as FIS, or CFTR activity measurements) display an improved dynamic range when performed using apical-out organoids.

In the recent years organoid cultures derived from tissue specific Lgr5+ adult stem cells emerged as novel models of organ development and disease [10,11]. By maintaining the activity of Wnt/β-Catenin signal transduction cascade – a key driver of most types of adult stem cells [12] – organoid cultures (OCs) can be grown *in vitro* for long-term in 3D extracellular matrix based hydrogels; whereas, epithelial cells in the culture maintain the original cellular diversity and organization of the organ of origin [13]. Originally small intestinal adult stem cells were used to generate crypt–villus like structures *in vitro* [14]. Since then OCs have been established from a wide range of organs in the gastrointestinal tract, including colon, esophagus [10], stomach [15], liver and pancreas [16]. Our group previously provided morphological and functional comparison of primary epithelial cells in mouse isolated ductal fragments and pancreatic organoid cultures. We demonstrated that the apical-to-basal polarity of the epithelial cells, gene and protein expressions and ion transport activities in the mouse pancreatic organoids remarkably overlap with those observed in freshly isolated primary ductal fragments [21]. These results highlighted that organoids are suitable to study epithelial cell functions as well. The previously published pancreatic organoid establishment protocol was based on manual picking of pancreatic ductal fragments after digesting the pancreatic tissue [32]. This step eventually requires manual work of pancreatic ductal fragment isolation and experience; which limit the throughput and hinder the automatization of the workflow. One significant innovation of the current study is the replacement of the manual picking of individual ductal fragments with an improved enzymatic digestion protocol of the whole pancreatic tissue, which improved the yield and success rate of organoid generation. The generated pancreatic organoids consisted solely of polarized epithelial cells and the success rate was 100%. The epithelial cells in the OCs expressed well-known ductal markers like CFTR, KRT19, SOX9, HNF1B or FOXA2, whereas non-ductal markers like amylase or insulin were completely absent. This suggests that our advanced technique is

suitable to generate pure pancreatic ductal cell cultures with high efficiency without the presence of other cell types. Another potential model to study pancreatic diseases is the human-induced pluripotent stem cells (hiPSCs) based organoids provide a unique platform for developmental studies and regenerative medicine [65]. The generation of pancreatic progenitor cells from PSCs is based on a sequential induction of definitive endoderm, foregut endoderm and pancreatic endoderm [66]. Although the differentiation of PSCs towards endocrine pancreatic progeny has been published [67], the generation of ductal and exocrine-like cells has not yet been adequately achieved. In a recent study Hohwieler et al developed a novel differentiation protocol and successfully generated human pancreatic acinar/ductal organoids from controls and cystic fibrosis patients that also recapitulated the defective CFTR function [68]. The cells in this culture also expressed acinar cell markers, such as amylase suggesting that it was a mixture of acinar and ductal cells. Recently the differentiation protocol was further developed, which improved the presence of pancreatic duct-like organoids [53]. The advantage of the currently published protocol is that it can provide pure ductal organoid cultures within a relatively short timeframe. Moreover, the elimination of the manual steps from the protocol may allow the automatization of the workflow for large scale manufacturing.

Another well-known limitation of the use of organoids is the ECMs such as Matrigel, that is essential for the growth of organoids, however, significantly reduces the applicable molecular biology toolset. ECM can limit the diffusion of the test compounds and pharmacons due to the molecular size and charge specificity of the individual molecules, whereas it hinders the application of siRNAs and plasmids. In addition, in the conventional organoid cultures the apical membrane of the epithelial cells is not directly accessible for drugs. Moreover, due to the vectorial transport of ions and fluid [9] the intraluminal pressure of the apical-in organoids is elevated without any pre-stimulation, which may affect the epithelial secretory processes [69]. To overcome these limitations, we induced the switch of the apical-to-basal polarity of the organoids by replacing the established organoids into an ECM-free suspension culture. Recently, Co et al. developed a technique to reverse enteroid polarity to study host-pathogen interactions [29]. They showed that apical-out enteroids maintain apical-to-basal polarity and barrier function in ECM-free media, differentiate into the major intestinal epithelial cell types, and exhibit polarized absorption of nutrients, whereas the bacterial entry mimics the *in vivo* entry process. The authors also demonstrated that the regulation of cell polarity by the ECM highly depends on the interaction of the ECM with β1 integrin, which acts as a receptor for ECM proteins. When the enteroids were treated with β1 integrin function-blocking antibody the polarity of BME-embedded enteroids reversed to an apical-out orientation. Notably, we

cannot rule out other ECM-β1 integrin independent factors in case of the pancreatic organoids, such as the increased intraluminal pressure. In our study immunostaining of CFTR, actin and occluding and visualization of the brush border on the outer surface of the apical-out organoids by scanning electron microscopy revealed a complete switch of the polarity after 48 h. This switch also led to a change of the epithelial cell morphology from an elongated to a cuboidal shape, suggesting that the elimination of the intraluminal pressure also affects the cell homeostasis. As an example, we demonstrated that the resting intracellular Ca^{2+} levels in unstimulated apical-out organoids were more consistent, compared to the apical-out organoids, whereas the intracellular Ca^{2+} release or extrusion was not changed. This finding may have a significant impact on the application of pancreatic organoids in different investigations, as the intracellular Ca^{2+} signaling determines the physiological secretion and pathological functions of the ductal cells [70]. It is important to emphasize that sustained elevation of the intracellular Ca^{2+} concentration leads to mitochondrial damage and impaired secretion of the ductal cells [71]. Notably, this property of the apical-out organoids may eliminate the interfere with the detectable effect of pharmacons acting on the intracellular Ca^{2+} signaling making this culture a preferential choice for such experiments. We also demonstrated that ductal epithelial cells express the mechanosensitive receptor Piezo1, which is a Ca^{2+} channel and senses the intraluminal pressure and stretch. PIEZO1 is also responsible for the induction of rapid epithelial cell division when it senses mechanical stretching thus regulating epithelial turnover, such as that caused by intraluminal pressure observed in apical-in organoids, which appears to be attenuated by polarity switching [72]. This was also confirmed by the decreased expression of the genes related to cell cycle in the apical-out organoids. Moreover Piezo1 also plays a critical role in transducing mechanical signals into an intracellular inflammatory cascade leading to tissue inflammation [73]. The activation of Piezo1 can regulate epithelial barrier functions negatively through Claudin-1 and induce epithelial dysfunction [28]. Notably, the polarity switch induced an increase in the expression of *MYO7*. Since *MYO7* is essentially responsible for the interaction between microvilli, its increased expression is presumably related to a decrease in luminal space and pressure, which could also account for the previously observed sparser microvilli density and size in mouse organoids compared to the patterns seen in the pressure draining tube-like primary isolated ducts [21]. Thus, the presence of intraluminal pressure in cystic organoids may therefore be a factor to be eliminated when comparing physiological and inflammatory conditions.

Next, we utilized the developed culture technique and the accessibility of apical membrane to investigate the ion transport of the polarized human pancreatic ductal cells. The current model

of pancreatic ductal HCO_3^- secretion is reviewed in detail elsewhere [1,74] . Briefly, the secretion of the large amount of HCO_3^- depends on the interaction of the SLC26A6 Cl^-/HCO_3^- exchanger and the CFTR Cl^- channel. SLC26A6 works with a $2HCO_3^-:1Cl^-$ stoichiometry, moreover the STAS domain of the SLC26A6 interacts with the R domain of CFTR leading to increased activation [10,75,76]. In addition, stimulation of the cells with cAMP agonists leads to an increased HCO_3^- permeability of CFTR and a marked drop of the intracellular Cl^- concentration [77]. This activates the WNK1-OSR1/SPAK pathway, that ultimately led to phosphorylation of CFTR and a marked increase in the relative permeability of CFTR to HCO_3^- [78]. In contrast to these, using our novel tool, we identified two ion channels that are expressed on the plasma membrane of the ductal cells and were never considered in pancreatic ion secretion. Our results revealed that ductal cells express functionally active ANO1, which is a Ca^{2+} activated Cl^- channel. ANO1 expression was only reported on the apical membrane of pancreatic acinar cells, in which HCO_3^- secretion via ANO1 attenuated the pH shift during acute pancreatitis [45]. In addition, we also demonstrated the expression and functional activity of ENaC on the apical membrane of the ductal cells. This was rather surprising, as researchers in the field agree, that ENaC does not participate in the pancreatic ductal functions, whereas it is widely expressed in many types of epithelial cells [79,80], mainly contributing to the reabsorption of luminal Na^+ and regulation of the volume and composition of the luminal fluid. Previous patch clamp studies on isolated rat ductal fragments showed no measurable effect of amiloride on ductal cells [42], which was not revised later in other species. Notably, our observations have potential limitations, that need to be considered when we interpret to physiological role of ENaC in the pancreas. First, pancreatic ductal cells located at the different parts of the ductal tree may exhibit different secretory activities. In the currently used model, we have no exact information which part of the ductal tree is represented in the organoid culture. In addition, the participation of these channels in the physiological secretory processes needs further evaluation. On the other hand, the introduction of two novel ion channels will require a detailed revision of the secretory process, that will remarkably improve the current model and should lead to a better understanding of the human exocrine pancreatic ion secretion **(Figure 31.)**. As both ENaC [80] and ANO1 [81] are considered potential therapeutic targets in CF and there is a significant interest to develop drugs that modify the channel function, these channels could also be capitalized in the treatment of exocrine pancreatic diseases, such as CF-related exocrine pancreatic insufficiency, or chronic pancreatitis [82,83].

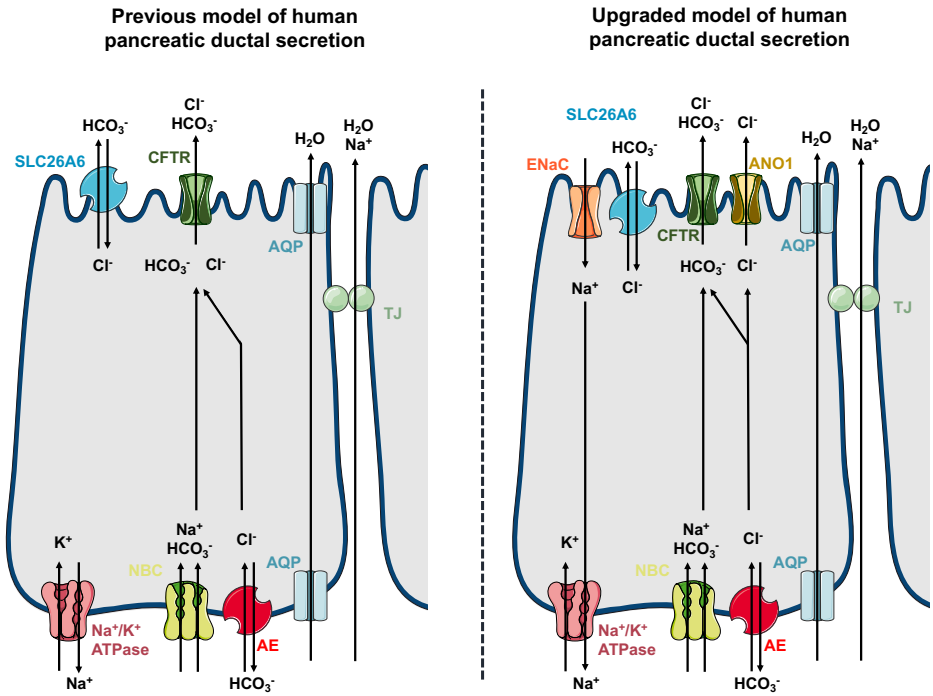

Figure 31. Comparison of the previous and our upgraded model of human pancreatic ductal cell secretion supplemented by novel findings reported in current thesis. Anion exchanger (AE), aquaporin (AQP), tight junction (TJ).

Finally, we provided examples, how this novel apical-out culture system could be used to improve the currently available functional assays. We demonstrated that the elimination of the intraluminal pressure remarkably improves the dynamic range of the FIS assay. FIS assay on human rectal organoids is used to predict drug response of CF patients [84]. In these screening assays researchers use rectal biopsy samples obtained from CF patients to generate organoid cultures to study the effect of CFTR correctors and predict drug response of the patients [85], whereas it may not be suitable in patients with remaining CFTR function [86]. The advantage of our approach is twofold, first, the elimination of the ECM could make the assay suitable for automatization and large-scale screening, second the improved dynamic range may lead to a better resolution of the results and higher precision of the clinical predictions. In addition, we also demonstrated that intracellular Cl^- measurements on apical-out organoids provide a better dynamic range and an improved dose-response of the ductal epithelial cells.

Taken together the results presented here go far beyond our current conclusions. By eliminating the intraluminal pressure in conventional organoids, we have not only gained information about the real capabilities of apical channels, but also opened the door to multi-field translational research. Polarity-switched human pancreatic organoids offer new options for regenerative therapies for diabetes, acute or chronic pancreatitis or for cystic fibrosis of the pancreas.

10. SUMMARY

Epithelial ion and fluid secretion determine the physiological functions of a broad range of organs, such as lung, liver, or pancreas. The molecular mechanism of pancreatic ion secretion is challenging to investigate due to the limited access to functional human ductal epithelia. Patient-derived organoids can overcome these limitations, but direct access to the apical membrane has not been achieved previously. Moreover, the previously used organoid generation technique requiring isolated pancreatic ducts, has limited the production of large quantities of organoids within a rational time frame, which limits their potential for high-throughput applications. In addition, due to the vectorial transport of ions and fluid the intraluminal pressure in the organoids is elevated, which may hinder the study of physiological processes.

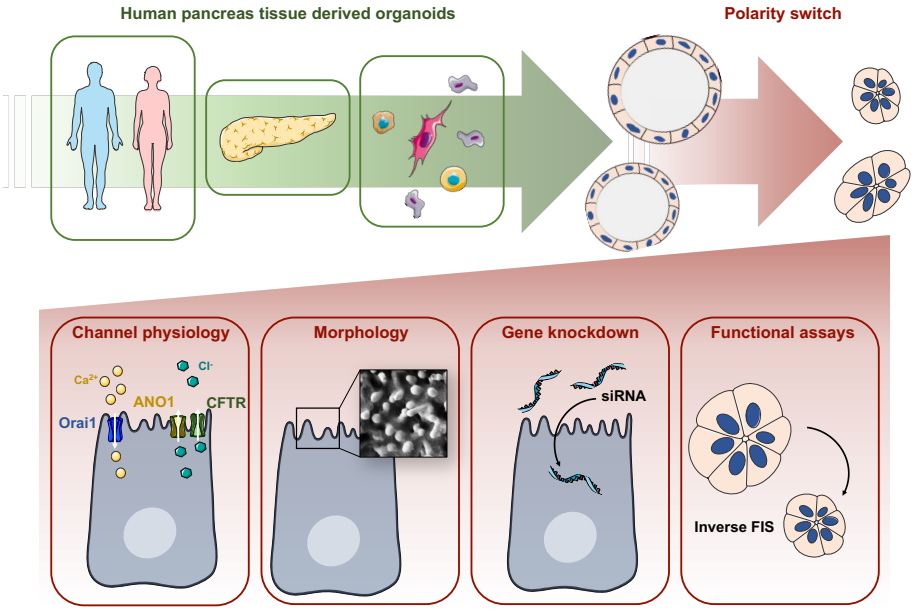

Figure 32. Summary figure of the expanded toolset achieved by polarity-switched human pancreatic ductal organoids.

To overcome these concerns, we first further optimized the cell isolation and tissue-derived organoid generation protocol, allowing the production of organoid cultures in large quantities without the manual isolation step of pancreatic ductal fragments. We also developed an advanced culturing method for human pancreatic organoids based on the removal of extracellular matrix that induced an apical-to-basal polarity switch also leading to reversed localization of proteins with polarized expression such as CFTR. ANO1 or ENaC. The cells in apical-out organoids had a cuboidal shape, whereas their resting intracellular Ca^{2+} concentration was more consistent compared to the cells in the apical-in organoids. Using this advanced model, which has been shown to be suitable for genetic perturbation techniques such as siRNA

gene silencing, we demonstrated the expression and function of two novel ion channels, the Ca^{2+} activated Cl^- channel Anoctamin 1 (ANO1) and the epithelial Na^+ channel (ENaC), which were not considered in ductal cells yet. Finally, we showed that the available functional assays, such as forskolin-induced swelling, or intracellular Cl^- measurement have improved dynamic range, when performed with apical-out organoids. Taken together our data suggest that polarity-switched human pancreatic ductal organoids are suitable models to expand our toolset in basic and translational research (**Figure 32.**).

11. SUMMARY OF NEW OBSERVATIONS

I. We have provided the evidence for human pancreatic ductal organoid culture establishment can be achieved by enzymatic tissue digestion without manual isolation of ductal fragments.

II. Production of organoid cultures showing pure epithelial identity in large quantities are also achieved by our optimized protocol.

III. We also developed an advanced culturing method for human pancreatic organoids based on the removal of extracellular matrix resulted in apical-to-basal polarity switch leading to reversed localization of proteins with polarized expression and directly accessible apical membrane surface in 3D cultures.

IV. We have also provided evidence that the essential component of OCs, the basement membrane matrix, Matrigel, which is blocking genetic perturbation procedures such as siRNA treatments in culture, can be routinely applied using apical-out organoids.

V. We demonstrated the expression and function of two novel ion channels, the Ca^{2+} activated Cl^- channel Anoctamin 1 (ANO1) and the epithelial Na^+ channel (ENaC), which were previously not considered in primary ductal cells.

VI. We have also shown that available functional assays such as forskolin-induced swelling or intracellular Cl^- measurement provide a better dynamic range when they are performed by using apical-out organoids.

12. ACKNOWLEDGMENTS

Ultimately, scientific progress is always a team effort, and I have had the privilege of learning this principle from the most inspiring people who have surrounded me all these years. Words cannot express my gratitude to my mentor and supervisor, **József Maléth,** for his support, guidance and friendship. Without his excellent supervision, this doctoral thesis and the rewarding years behind it would not have been accomplished.

I am grateful to **Prof. Dr Csaba Lengyel,** the current head of the Department of Internal Medicine, who gave me the opportunity to work in his department. My sincere gratitude is owed to **Dr Petra Pallagi** for her cooperation, help, valuable insights, and friendship throughout these years.

I would like to express my deepest appreciation to those with whom we have accompanied each other on this journey, **Tamara Madácsy, Viktória Szabó, Boldizsár Jójárt, Aletta Kiss, Petra Susánszki, Noémi Papp.** I'm grateful for all your help, encouragement, and the great times we had together, without their inspiration, this project would not have been possible.

I am deeply grateful to all of my colleagues who have taught, helped and supported me over the years, **Tünde Molnár, Tim Crul, Bálint Tél, Ingrid Hegnes Sendstad, Marietta Görög, Krisztina Dudás, Melinda Molnár, Zsuzsanna Konczos, Edit Magyarné Pálfi, Tünde Pritz, Rea Fritz, Zsuzsa Árva**.

I could not have undertaken this journey without my beloved patient and encouraging friends who have stood by me all along, **Klaudia Kocsy, Dorottya Szabó, Péter Gaál, Kata Sárközi, Nikolett Kiss, Eszmeralda Ney, István Kelle**, thank you for all your support.

Last but not least, I am most grateful for the sacrifices of those who have never ceased to support me on the road to my choice towards academic achievements. I owe warm thanks to my amazing mom **Edit Répási**, my dad **László Varga** and my brother **Tamás Varga**. You were the shield that never let me down but protected me while I dedicated myself to science. I can never be thankful enough for your efforts.

13. REFERENCES

1. Lee, M. G., Ohana, E., Park, H. W., Yang, D. & Muallem, S. Molecular mechanism of pancreatic and salivary gland fluid and HCO3 secretion. *Physiol. Rev.* **92**, 39–74 (2012).
2. Hegyi, P., Pandol, S., Venglovecz, V. & Rakonczay, Z. The acinar-ductal tango in the pathogenesis of acute pancreatitis. *Gut* **60**, 544–552 (2011).
3. Pallagi, P. *et al.* Trypsin reduces pancreatic ductal bicarbonate secretion by inhibiting CFTR Cl^- channels and luminal anion exchangers. *Gastroenterology* **141**, 2228-2239.e6 (2011).
4. Pallagi, P. *et al.* The role of pancreatic ductal secretion in protection against acute pancreatitis in mice*. *Crit. Care Med.* **42**, e177-188 (2014).
5. Zeng, M. *et al.* Restoration of CFTR Activity in Ducts Rescues Acinar Cell Function and Reduces Inflammation in Pancreatic and Salivary Glands of Mice. *Gastroenterology* **153**, 1148–1159 (2017).
6. Madácsy, T., Pallagi, P. & Maleth, J. Cystic Fibrosis of the Pancreas: The Role of CFTR Channel in the Regulation of Intracellular Ca2+ Signaling and Mitochondrial Function in the Exocrine Pancreas. *Front. Physiol.* **9**, (2018).
7. Fűr, G. *et al.* Mislocalization of CFTR expression in acute pancreatitis and the beneficial effect of VX-661 + VX-770 treatment on disease severity. *J. Physiol.* **599**, 4955–4971 (2021).
8. Hegyi, P. *et al.* CFTR: A new horizon in the pathomechanism and treatment of pancreatitis. *Rev. Physiol. Biochem. Pharmacol.* **170**, 37–66 (2016).
9. Ahuja, M., Jha, A., Maléth, J., Park, S. & Muallem, S. cAMP and Ca2+ signaling in secretory epithelia: Crosstalk and synergism. *Cell Calcium* **55**, 385–393 (2014).
10. Ko, S. B. H. *et al.* Gating of CFTR by the STAS domain of SLC26 transporters. *Nat. Cell Biol.* **6**, 343–350 (2004).
11. Horvath, P. *et al.* Screening out irrelevant cell-based models of disease. *Nat. Rev. Drug Discov.* **15**, 751–769 (2016).
12. Cheng, H. S. *et al.* Concurrent and Independent HCO^-3 and Cl^- Secretion in a Human Pancreatic Duct Cell Line (CAPAN-1). *J. Membr. Biol.* **164**, 155–167 (1998).
13. Maléth, J. *et al.* Alcohol disrupts levels and function of the cystic fibrosis transmembrane conductance regulator to promote development of pancreatitis. *Gastroenterology* **148**, 427-439.e16 (2015).
14. Wang, J., Haanes, K. A. & Novak, I. Purinergic regulation of CFTR and Ca^{2+} -activated Cl^- channels and K^+ channels in human pancreatic duct epithelium. *Am. J. Physiol.-Cell Physiol.* **304**, C673–C684 (2013).
15. Argent, B. E., Arkle, S., Cullen, M. J. & Green, R. Morphological, biochemical and secretory studies on rat pancreatic ducts maintained in tissue culture. *Q. J. Exp. Physiol. Camb. Engl.* **71**, 633–648 (1986).
16. Maléth, J. *et al.* Non-conjugated chenodeoxycholate induces severe mitochondrial damage and inhibits bicarbonate transport in pancreatic duct cells. *Gut* **60**, 136–138 (2011).
17. Fanczal, J. *et al.* TRPM2-mediated extracellular Ca2+ entry promotes acinar cell necrosis in biliary acute pancreatitis. *J. Physiol.* **598**, 1253–1270 (2020).
18. Pallagi, P. *et al.* Bile acid- and ethanol-mediated activation of Orai1 damages pancreatic ductal secretion in acute pancreatitis. *J. Physiol.* JP282203 (2022) doi:10.1113/JP282203.
19. Tél, B. *et al.* Thiopurines impair the apical plasma membrane expression of CFTR in pancreatic ductal cells via RAC1 inhibition. *Cell. Mol. Life Sci.* **80**, 31 (2023).
20. Yui, S. *et al.* Functional engraftment of colon epithelium expanded in vitro from a single adult Lgr5+ stem cell. *Nat. Med.* **18**, 618–623 (2012).
21. Molnár, R. *et al.* Mouse pancreatic ductal organoid culture as a relevant model to study

exocrine pancreatic ion secretion. *Lab. Invest.* **100**, 84–97 (2020).
22. Bakhti, M. *et al.* Establishment of a high-resolution 3D modeling system for studying pancreatic epithelial cell biology in vitro. *Mol. Metab.* **30**, 16–29 (2019).
23. Sato, T. *et al.* Single Lgr5 stem cells build crypt-villus structures in vitro without a mesenchymal niche. *Nature* **459**, 262–265 (2009).
24. Clevers, H. Modeling Development and Disease with Organoids. *Cell* **165**, 1586–1597 (2016).
25. Sachs, N. *et al.* Long-term expanding human airway organoids for disease modeling. *EMBO J.* **38**, e100300 (2019).
26. Georgakopoulos, N. *et al.* Long-term expansion, genomic stability and in vivo safety of adult human pancreas organoids. *BMC Dev. Biol.* **20**, 4 (2020).
27. Huch, M. *et al.* Long-term culture of genome-stable bipotent stem cells from adult human liver. *Cell* **160**, 299–312 (2015).
28. Jiang, Y. *et al.* Piezo1 regulates intestinal epithelial function by affecting the tight junction protein claudin-1 via the ROCK pathway. *Life Sci.* **275**, 119254 (2021).
29. Co, J. Y. *et al.* Controlling Epithelial Polarity: A Human Enteroid Model for Host-Pathogen Interactions. *Cell Rep.* **26**, 2509-2520.e4 (2019).
30. Co, J. Y., Margalef-Català, M., Monack, D. M. & Amieva, M. R. Controlling the polarity of human gastrointestinal organoids to investigate epithelial biology and infectious diseases. *Nat. Protoc.* **16**, 5171–5192 (2021).
31. Stroulios, G. *et al.* Apical-out airway organoids as a platform for studying viral infections and screening for antiviral drugs. *Sci. Rep.* **12**, 7673 (2022).
32. Boj, S. F. *et al.* Organoid models of human and mouse ductal pancreatic cancer. *Cell* **160**, 324–338 (2015).
33. Shik Mun, K. *et al.* Patient-derived pancreas-on-a-chip to model cystic fibrosis-related disorders. *Nat. Commun.* **10**, 3124 (2019).
34. Feraille, E. & Dizin, E. Coordinated Control of ENaC and Na+,K+-ATPase in Renal Collecting Duct. *J. Am. Soc. Nephrol. JASN* **27**, 2554–2563 (2016).
35. Noreng, S., Bharadwaj, A., Posert, R., Yoshioka, C. & Baconguis, I. Structure of the human epithelial sodium channel by cryo-electron microscopy. *eLife* **7**, e39340 (2018).
36. Berdiev, B. K., Qadri, Y. J. & Benos, D. J. Assessment of the CFTR and ENaC association. *Mol. Biosyst.* **5**, 123–127 (2009).
37. Moore, P. J. & Tarran, R. The epithelial sodium channel (ENaC) as a therapeutic target for cystic fibrosis lung disease. *Expert Opin. Ther. Targets* **22**, 687–701 (2018).
38. Kunzelmann, K., Schreiber, R., Nitschke, R. & Mall, M. Control of epithelial Na+ conductance by the cystic fibrosis transmembrane conductance regulator. *Pflugers Arch.* **440**, 193–201 (2000).
39. Catalán, M. A. *et al.* Cftr and ENaC ion channels mediate NaCl absorption in the mouse submandibular gland. *J. Physiol.* **588**, 713–724 (2010).
40. Waldmann, R., Champigny, G., Bassilana, F., Voilley, N. & Lazdunski, M. Molecular cloning and functional expression of a novel amiloride-sensitive Na+ channel. *J. Biol. Chem.* **270**, 27411–27414 (1995).
41. McDonald, F. J., Snyder, P. M., McCray, P. B. & Welsh, M. J. Cloning, expression, and tissue distribution of a human amiloride-sensitive Na+ channel. *Am. J. Physiol.* **266**, L728-734 (1994).
42. Novak, I. & Hansen, M. R. Where have all the Na+ channels gone? In search of functional ENaC in exocrine pancreas. *Biochim. Biophys. Acta* **1566**, 162–168 (2002).
43. Caputo, A. *et al.* TMEM16A, a membrane protein associated with calcium-dependent chloride channel activity. *Science* **322**, 590–594 (2008).
44. Yang, Y. D. *et al.* TMEM16A confers receptor-activated calcium-dependent chloride

conductance. *Nature* **455**, 1210–1215 (2008).
45. Han, Y., Shewan, A. M. & Thorn, P. HCO3- Transport through Anoctamin/Transmembrane Protein ANO1/TMEM16A in Pancreatic Acinar Cells Regulates Luminal pH. *J. Biol. Chem.* **291**, 20345–20352 (2016).
46. Edlund, A., Esguerra, J. L. S., Wendt, A., Flodström-Tullberg, M. & Eliasson, L. CFTR and Anoctamin 1 (ANO1) contribute to cAMP amplified exocytosis and insulin secretion in human and murine pancreatic beta-cells. *BMC Med.* **12**, 87 (2014).
47. Jung, J. *et al.* Dynamic modulation of ANO1/TMEM16A HCO3(-) permeability by Ca2+/calmodulin. *Proc. Natl. Acad. Sci. U. S. A.* **110**, 360–365 (2013).
48. Guo, S., Zhang, L. & Li, N. ANO1: More Than Just Calcium-Activated Chloride Channel in Cancer. *Front. Oncol.* **12**, 922838 (2022).
49. Liu, Y., Liu, Z. & Wang, K. The Ca2+-activated chloride channel ANO1/TMEM16A: An emerging therapeutic target for epithelium-originated diseases? *Acta Pharm. Sin. B* **11**, 1412–1433 (2021).
50. Madácsy, T. *et al.* Impaired regulation of PMCA activity by defective CFTR expression promotes epithelial cell damage in alcoholic pancreatitis and hepatitis. *Cell. Mol. Life Sci.* **79**, 265 (2022).
51. Mödl, B., Schmidt, K., Moser, D. & Eferl, R. The intermicrovillar adhesion complex in gut barrier function and inflammation. *Explor. Dig. Dis.* 72–79 (2022) doi:10.37349/edd.2022.00006.
52. Kwon, O., Han, T.-S. & Son, M.-Y. Intestinal Morphogenesis in Development, Regeneration, and Disease: The Potential Utility of Intestinal Organoids for Studying Compartmentalization of the Crypt-Villus Structure. *Front. Cell Dev. Biol.* **8**, (2020).
53. Breunig, M. *et al.* Modeling plasticity and dysplasia of pancreatic ductal organoids derived from human pluripotent stem cells. *Cell Stem Cell* **28**, 1105-1124.e19 (2021).
54. Ahuja, M., Chung, W. Y., Lin, W.-Y., McNally, B. A. & Muallem, S. Ca2+ Signaling in Exocrine Cells. *Cold Spring Harb. Perspect. Biol.* **12**, a035279 (2020).
55. Kunisaki, C. Role of the Anoctamin Family in Various Carcinomas. *Ann. Surg. Oncol.* **27**, 3112–3114 (2020).
56. Berg, J., Yang, H. & Jan, L. Y. Ca2+-activated Cl− channels at a glance. *J. Cell Sci.* **125**, 1367–1371 (2012).
57. Ferrera, L., Zegarra-Moran, O. & Galietta, L. J. V. Ca2+-activated Cl- channels. *Compr. Physiol.* **1**, 2155–2174 (2011).
58. Lin, H., Roh, J., Woo, J. H., Kim, S. J. & Nam, J. H. TMEM16F/ANO6, a Ca2+-activated anion channel, is negatively regulated by the actin cytoskeleton and intracellular MgATP. *Biochem. Biophys. Res. Commun.* **503**, 2348–2354 (2018).
59. Gray, M. A., Winpenny, J. P., Porteous, D. J., Dorin, J. R. & Argent, B. E. CFTR and calcium-activated chloride currents in pancreatic duct cells of a transgenic CF mouse. *Am. J. Physiol.* **266**, C213-221 (1994).
60. Enuka, Y., Hanukoglu, I., Edelheit, O., Vaknine, H. & Hanukoglu, A. Epithelial sodium channels (ENaC) are uniformly distributed on motile cilia in the oviduct and the respiratory airways. *Histochem. Cell Biol.* **137**, 339–353 (2012).
61. Khedr, S. *et al.* Increased ENaC activity during kidney preservation in Wisconsin solution. *BMC Nephrol.* **20**, 145 (2019).
62. Canessa, C. M., Merillat, A. M. & Rossier, B. C. Membrane topology of the epithelial sodium channel in intact cells. *Am. J. Physiol.* **267**, C1682-1690 (1994).
63. Baldin, J.-P., Barth, D. & Fronius, M. Epithelial Na+ Channel (ENaC) Formed by One or Two Subunits Forms Functional Channels That Respond to Shear Force. *Front. Physiol.* **11**, (2020).
64. Dekkers, J. F. *et al.* A functional CFTR assay using primary cystic fibrosis intestinal

organoids. *Nat. Med.* **19**, 939–945 (2013).
65. Xu, X. *et al.* Dppa3 expression is critical for generation of fully reprogrammed iPS cells and maintenance of Dlk1-Dio3 imprinting. *Nat. Commun.* **6**, 6008 (2015).
66. Xie, R. *et al.* Dynamic chromatin remodeling mediated by polycomb proteins orchestrates pancreatic differentiation of human embryonic stem cells. *Cell Stem Cell* **12**, 224–237 (2013).
67. Rezania, A. *et al.* Reversal of diabetes with insulin-producing cells derived in vitro from human pluripotent stem cells. *Nat. Biotechnol.* **32**, 1121–1133 (2014).
68. Hohwieler, M. *et al.* Human pluripotent stem cell-derived acinar/ductal organoids generate human pancreas upon orthotopic transplantation and allow disease modelling. *Gut* **66**, 473–486 (2017).
69. Spelier, S. *et al.* High-throughput functional assay in cystic fibrosis patient-derived organoids allows drug repurposing. *ERJ Open Res.* **9**, 00495–02022 (2023).
70. Maléth, J. & Hegyi, P. Calcium signaling in pancreatic ductal epithelial cells: an old friend and a nasty enemy. *Cell Calcium* **55**, 337–345 (2014).
71. Maléth, J. & Hegyi, P. Ca2+ toxicity and mitochondrial damage in acute pancreatitis: translational overview. *Philos. Trans. R. Soc. Lond. B. Biol. Sci.* **371**, 20150425 (2016).
72. Gudipaty, S. A. *et al.* Mechanical stretch triggers rapid epithelial cell division through Piezo1. *Nature* **543**, 118–121 (2017).
73. Liu, H. *et al.* Piezo1 Channels as Force Sensors in Mechanical Force-Related Chronic Inflammation. *Front. Immunol.* **13**, (2022).
74. Saint-Criq, V. & Gray, M. A. Role of CFTR in epithelial physiology. *Cell. Mol. Life Sci.* **74**, 93–115 (2017).
75. Wang, Y. *et al.* Slc26a6 regulates CFTR activity in vivo to determine pancreatic duct HCO3− secretion: relevance to cystic fibrosis. *EMBO J.* **25**, 5049–5057 (2006).
76. Sohma, Y., Gray, M. A., Imai, Y. & Argent, B. E. HCO3− Transport in a Mathematical Model of the Pancreatic Ductal Epithelium. *J. Membr. Biol.* **176**, 77–100 (2000).
77. Ishiguro, H. *et al.* Chloride transport in microperfused interlobular ducts isolated from guinea-pig pancreas. *J. Physiol.* **539**, 175–189 (2002).
78. Park, H. W. *et al.* Dynamic Regulation of CFTR Bicarbonate Permeability by [Cl−]i and Its Role in Pancreatic Bicarbonate Secretion. *Gastroenterology* **139**, 620–631 (2010).
79. Kunzelmann, K. & Mall, M. Electrolyte transport in the mammalian colon: mechanisms and implications for disease. *Physiol. Rev.* **82**, 245–289 (2002).
80. Mall, M. A. ENaC inhibition in cystic fibrosis: potential role in the new era of CFTR modulator therapies. *Eur. Respir. J.* **56**, 2000946 (2020).
81. Galietta, L. J. V. TMEM16A (ANO1) as a therapeutic target in cystic fibrosis. *Curr. Opin. Pharmacol.* **64**, 102206 (2022).
82. Madácsy, T., Pallagi, P. & Maleth, J. Cystic Fibrosis of the Pancreas: The Role of CFTR Channel in the Regulation of Intracellular Ca2+ Signaling and Mitochondrial Function in the Exocrine Pancreas. *Front. Physiol.* **9**, 1585 (2018).
83. Kleeff, J. *et al.* Chronic pancreatitis. *Nat. Rev. Dis. Primer* **3**, 17060 (2017).
84. Muilwijk, D. *et al.* Forskolin-induced Organoid Swelling is Associated with Long-term CF Disease Progression. *Eur. Respir. J.* 2100508 (2022) doi:10.1183/13993003.00508-2021.
85. Vonk, A. M. *et al.* Protocol for Application, Standardization and Validation of the Forskolin-Induced Swelling Assay in Cystic Fibrosis Human Colon Organoids. *STAR Protoc.* **1**, 100019 (2020).
86. Boj, S. F. *et al.* Forskolin-induced Swelling in Intestinal Organoids: An In Vitro Assay for Assessing Drug Response in Cystic Fibrosis Patients. *J. Vis. Exp. JoVE* 55159 (2017) doi:10.3791/55159.